INFORMATION TO USERS

This manuscript has been reproduced from the microfilm master. UMI films the text directly from the original or copy submitted. Thus, some thesis and dissertation copies are in typewriter face, while others may be from any type of computer printer.

The quality of this reproduction is dependent upon the quality of the copy submitted. Broken or indistinct print, colored or poor quality illustrations and photographs, print bleedthrough, substandard margins, and improper alignment can adversely affect reproduction.

In the unlikely event that the author did not send UMI a complete manuscript and there are missing pages, these will be noted. Also, if unauthorized copyright material had to be removed, a note will indicate the deletion.

Oversize materials (e.g., maps, drawings, charts) are reproduced by sectioning the original, beginning at the upper left-hand corner and continuing from left to right in equal sections with small overlaps.

ProQuest Information and Learning
300 North Zeeb Road, Ann Arbor, MI 48106-1346 USA
800-521-0600

Alternative Code Acquisition Methods for WCDMA Systems

Hui Zhang

A Thesis

in

The Department

of

Electrical and Computer Engineering

Presented in Partial Fulfillment of the Requirements

for the Degree of Master of Applied Science at

Concordia University

Montréal, Québec, Canada

Feb 2002

ABSTRACT

Alternative Code Acquisition Methods for WCDMA Systems

In a CDMA cellular system, the process of the mobile station searching for a cell and achieving code and time synchronization to its downlink scrambling code is referred to as cell search. In WCDMA, the cell search is divided into five acquisition stages: slot synchronization, frame synchronization and scrambling code group identification, scrambling code identification, frequency acquisition, and cell identification. A pipelined process of the first three stages minimizes the average code and acquisition time. This report presents algorithms and results for serial search and pipeline search. The acquisition times in different cases are compared. We present six policies. A simulation testbed is used to compare the performance of the six algorithms. It is shown from the simulation results that system performance is greatly improved by using modified cell search. Our WCDMA algorithms is shown to outperform the other algorithms in all of the test situations considered (e.g., AWGN channel, four types of fading channels). In addition, our algorithm requires less time to get code acquisition than the other algorithms.

Dedicated to my dearest parents .....

ACKNOWLEDGEMENTS

I would like to thank my academic advisor, Dr. Ahmed K. Elhakeem, for the invaluable support, guidance and encouragement he has provided over the past year.

I would like to thank all my friends who have provided me all kinds of help in the last two years.

Most of all, I would like to thank my parents for their love and encouragement. I could not have completed my degree without their continuous and immeasurable support.

TABLE OF CONTENTS

LIST OF TABLES

LIST OF FIGURES

Chapter 1

Introduction

The goal for the next generation of mobile communications system is to seamlessly provide a wide variety of communication services to anybody, anywhere, anytime. The intended service for next generation mobile phone users include services like transmitting high speed data, video and multimedia traffic as well as voice signals. The technology needed to tackle the challenges to make these services available is popularly known as Third Generation (3G) Cellular Systems. The first generation systems are represented by the analog mobile systems designed to carry the voice application traffic. Their subsequent digital counterparts are known as second generation cellular systems. Third generation systems mark a significant leap, both in applications and capacity, from the current second generation standards. Whereas the current digital mobile phone systems are optimized for voice communications, 3G communicators are oriented towards multimedia message capability.

1.1 First Generation Cellular Systems

The first generation cellular systems generally employ analog Frequency Modulation (FM) techniques. The Advanced Mobile Phone System (AMPS)[1] is the most notable of the first generation systems. AMPS was developed by the Bell Telephone

System. It uses FM technology for voice transmission and digital signaling for control information. Other first generation systems include:

- Narrow band AMPS [2](NAMPS)
- Total Access Cellular System (TACS)
- Nordic Mobile Telephone System[3] (NMT-900)

All the first generation cellular systems employ Frequency Division Multiple Access (FDMA) with each channel assigned to a unique frequency band within a cluster of cells.

1.2 Second Generation Cellular Systems

The rapid growth in the number of subscribers and the proliferation of many incompatible first generation systems were the main reason behind the evolution towards second generation cellular systems. Second generation systems take advantage of compression and coding techniques associated with digital technology. All the second generation systems employ digital modulation schemes. Multiple access techniques like Time Division Multiple Access (TDMA) and Code Division Multiple Access (CDMA) are used along with FDMA[4] in the second generation systems. Second generation cellular systems include:

- United States Digital Cellular (USDC) standards IS-54 and IS-136
- Global System for Mobile communications (GSM)
- Pacific Digital Cellular (PDC)[7]
- cdmaOne

1.3 Third Generation Cellular Systems

Third generation cellular systems are being designed to support wide band services like high speed Internet access, video and high quality image transmission with the same quality as the fixed networks. The primary requirements of the next generation cellular systems are [5]:

- Voice quality comparable to Public Switched Telephone Network (PSTN).[6]
- Support of high data rate. The following table shows the data rate requirement of the 3G systems

Table 1.1: 3G Data Rate Requirements

Mobility	Minimum
Vehicular	144 kbps
Outdoor to indoor and pedestrian	384 kbps
Indoor Office	2 Mbps

- Support of both packet-switched and circuit-switched data services.
- More efficient usage of the available radio spectrum
- Support of a wide variety of mobile equipment
- Backward with pre-existing networks and flexibility to permit the introduction of new services and technology
- An adaptive radio interface suited to the highly asymmetric nature of most Internet communications: a much greater bandwidth for the down link than the up link.

1.4 WCDMA: Air Interface for 3G

One of the most promising approaches to 3G is to combine a Wideband CDMA (WCDMA) air interface with the fixed network of GSM. Several proposals supporting WCDMA were submitted to the International Telecommunication Union (ITU) and its International Mobile Telecommunications for the year 2000 (IMT2000) initiative for 3G. Among several organizations trying to merge their various WCDMA proposals are:

- Japan Association of Radio Industry and Business (ARIB)
- Alliance for Telecommunications Industry Solutions[7] (ATIS)
- European Telecommunications Standards Institute (ETSI) through its Special Mobile Group (SMG)

All these schemes try to take advantage of the WCDMA radio techniques without ignoring the numerous advantages of the already existing GSM networks. The standard that has emerged is based on ETSIs Universal Mobile Telecommunication System (UMTS) and is commonly known as UMTS Terrestrial Radio Access (UTRA) [8]. The access scheme for UTRA is Direct Sequence Code Division Multiple Access (DS-CDMA). The information is spread over a band of approximately 5 MHz. This wide bandwidth has given rise to the name Wideband CDMA or WCDMA. There are two different modes namely:

- Frequency Division Duplex (FDD)
- Time Division Duplex (TDD)

Since different regions have different frequency allocation schemes, the capability to operate in either FDD or TDD mode allows for efficient utilization of the available spectrum.

1.4.1 WCDMA Key Features

The key operational features of the WCDMA radio interface are listed below [1], [10]:

- Support of high data rate transmission: 384 kbps with wide area coverage, 2 Mbps with local coverage.
- High service flexibility: support of multiple parallel variable rate services on each connection.
- Both Frequency Division Duplex (FDD)[11] and Time Division Duplex (TDD)[11].
- Built in support for future capacity and coverage enhancing technologies like adaptive antennas, advanced receiver structures and transmitter diversity.
- Support of inter frequency hand over and hand over to other systems, including hand over to GSM.
- Efficient packet access.

1.4.2 WCDMA Key Technical Characteristics

The following table shows the key technical features of the WCDMA radio interface:

Table 1.2: WCDMA Key Technical Characteristics

Multiple Access Scheme	DS-CDMA
Duplex Scheme	FDD/TDD
Packet Access	Dual mode (Combined and Dedicated Channel)
Multirate/Variable rate scheme	Variable spreading factor and multi-code
Chip Rate	3.84 Mcps
Carrier Spacing	4.4-5.2Mhz (200 kHZ carrier raster)
Frame Length	10ms
Inter Base Station Synchronization	FDD: No accurate synchronization needed
	TDD: Synchronization required
Channel Coding Scheme	Convolution Code (rate 1/2 and 1/3) Turbo code

The chip rate may be extended to two or three times the standard 3.84 Mcps to accommodate for data rates higher than 2 Mbps. The 200 kHz carrier difference has been chosen to facilitate coexistence and inter operability with GSM.

Chapter 2

Code Acquisition Schemes

2.1 Introduction

In spread-spectrum communication, the receive spread waveform, generated replica of the spreading waveform and initially synchronized in both phase and frequency. So initial spreading waveform synchronization is an extremely important problem in spread-spectrum. In fact, overall system performance is often limited by the performance of the synchronizer. The simplest synchronization scheme is to sweep the receiver spreading waveform phase until the proper phase is sensed. Stepped serial search over all potential waveform phases will usually achieve lower synchronization times than the sweep search. After each phase step in a stepped serial search system, the correctness of the phase must be evaluated. This is accomplished by attempting to despread the received waveform using the trial spreading waveform phase. When the phase is correct, the input signal spectrum is collapsed and energy appears at the output of a narrow-band filter.

The primary function of a direct sequence (DS)[12] spread spectrum receiver is to despread the received pseudo-noise (PN)[13] code. The process involves generating a local replica of the PN code in the receiver and then synchronizing this local PN signal to the received one. The process of synchronizing the local and received

PN signals is accomplished in two stages. Initially, a coarse alignment of the two PN signals is produced within a small residual relative timing offset. This process make incoming PN code acquired, a fine synchronization system takes over and continuously maintains the best possible waveform alignment by means of a closed loop operation. The process of maintaining the two codes in fine synchronism is referred to as PN tracking.

2.2 Serial search

A widely used technique for initial synchronization is to search serially through all potential code phases and frequencies until the correct phase and frequency are identified. Each reference phase/frequency is evaluated by attempting to despread the received signal. If the estimated code phase and frequency are correct, despreading will occur and will be sensed. If the estimated code phase or frequency is incorrect, the received signal will not be despread, and the reference waveform will be stepped to a new phase/frequency for evaluation. This technique is called serial search. There are two important probabilities in this scheme, one is P_{fa}, the probability of false alarm, the other is P_d, the probability of correct detection. They are both a function of evaluation (integration) time and signal to noise ratio.

Serial search acquisition schemes have been referred to as low decision rate detectors since a large number of spreading code symbols must typically be received to make a correct/incorrect decision on the hypothesized reference spreading code phase/frequency.

This intial synchronization of the spreading waveforms is a significant problem in spread-spectrum system design. Phase/frequency synchronization is difficult because typical spreading waveform periods are long and bandwidths are large. Thus uncertainty in the estimated propagation delay T_d translates into a large number of symbols of code phase uncertainty which must also be resolved. The correct code

phase/frequency must be found quickly using the minimum amount of hardware possible.

Serial search techniques are by far the most commonly used spread spectrum synchronization techniques. Inputs to the mean synchronization time computation are the probability of detection when the correct cells being evaluated P_d, and the probability of detection when the correct cells being evaluated, P_{fa}, as a function of the integration time T_i and SNR.

For simplicity assume that no frequency uncertainty exists and that the correct phase is uniformly distributed over the region ΔT. Based on the spreading waveform autocorrelation function, a phase step size of Δt seconds has been chosen. For convenience assume that $\Delta T/\Delta t$ is an integer C. Because it is equally probable that the correct phase is in any cell, the serial search can begin anywhere. Let the search begin at one boundary of the uncertainty region. The search will advance through one cell at a time until C cells have been evaluated. If synchronization has not been achieved at that time, a retrace will start the search over again.

The mean synchronization time is calculated in a straightforward manner considering all possible sequences of events leading to a correct synchronization. An event in the probability space being considered is defined by a particular location n for the correct phase cell, a particular number of missed detections j of the correct phase cell, and a particular number of false alarms k in all incorrect phase cells evaluated. The total synchronization time for a particular event defined by (n,j,k)[14] is :

$$T(n,j,k) = nT_i + jCT_i + kT_{fa}$$

where T_i is the (fixed) integration time for the evaluation of each cell and T_{fa} is the time required to reject an incorrect cell when a false alarm occurs. The

false alarm penalty T_{fa} may be many times larger than T_i, so that false alarms are undesirable events. The total number of cells evaluated for this event is (n−jC), the total number of correct cells is (j−1), and the total number of incorrect cells is (n−jC-j-1). The probability of the correct cell being the nth cell is 1/C and the probability of j missed detections followed by a correct detection is $P_d\ (1\text{-}P_d)^j$. P_d is geometrically distribution. The k false alarms can occur in any order within the (n+jC-j-1)≅ K[14] incorrect cells. The probability of a particular ordering is $P_{fa}^k(1-P_{fa})^{K-k}$, and there are $\begin{pmatrix} K \\ k \end{pmatrix}$ orderings of k false alarms in K cells. Combining all of the above, the probability of the event (n,j,k) is

$$P_r(n,j,k) = \frac{1}{C}P_d(1-P_d)^j \begin{pmatrix} K \\ k \end{pmatrix} P_{fa}^k(1-P_{fa})^{K-k}$$

The mean synchronization time is

$$T_s = \sum_{n,j,k} T(n,j,k)P_r(n,j,k)$$

The correct cell number can range over(1,C), the number of missed detection can range from zero to infinity, and the number of false alarms ranges over (0,K). Thus the mean synchronization time is

$$T_s = \frac{1}{C}\sum_{n=1}^{C}\sum_{j=0}^{\infty}[(n+jC)T_i + KT_{fa}P_{fa}]\,P_d(1-P_d)^J$$

The result is

$$T_s = (C-1)T_{da}\left(\frac{2-P_d}{2P_d}\right) + \frac{T_i}{P_d}$$

where

$$T_{da} = T_i + T_{fa}P_{fa}$$

T_{da} is the average dwell time at an incorrect phase cell.

If we know the probability density function of the envolope detector output, we can caculate the probability of detector and the probability of the fasle alarm.The probability of detection is the integral from V_t to infinity of this pdf evaluated for the maximum signal-to-noise ratio[15]. Probability of false alarm is the same integral evaluated at the minimum signal-to-noise ratio(i.e, for A=0). These calculations are depicted graphically in Fig 2.1, which shows the pdf for SNRs of zero and eight. The area which is crosshatched is P_d and the area which is double crosshatched is P_{fa}. Both P_d and P_{fa} are functions of SNR and V_t and can not be independently selected. For a specific SNR, the selection of P_{fa} implies a particular threshold V_t which then sets P_d . Fig 2.1 illustrates these relationships.

2.2.1 Single-dwell serial acquisition

A simple model of a single dwell serial PN acquisition system is illustrated in Fig.2.3 The model employs a standard type, non-coherent(square-law) detector[16]. Briefly, the received signal plus noise is actively correlated with a local replica of the PN code and passed through a bandpass filter. The output of the filter is then square-law envelope detected with the detector output being integrated for a fixed time duration, τ_d (the dwell time), and then compared to a preset threshold.

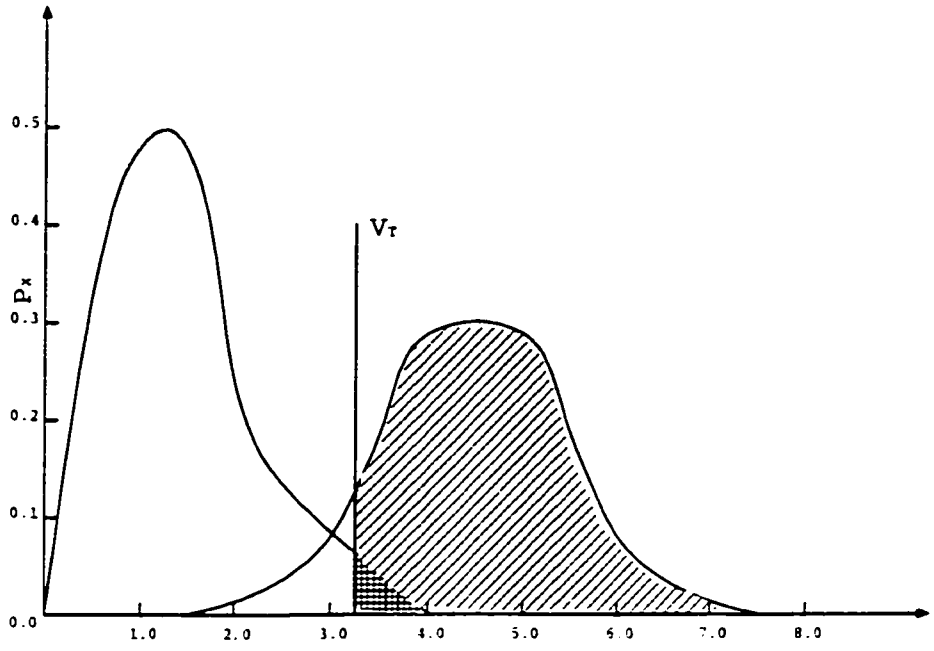

Figure 2.1: Example of the calculation of P_d and P_{fa}

2.2.1.1 State-transition Diagram

The state- transition diagram is also called a Markov Chain[17]. We use this to illustrate the acquisition process. If the detector output is above the preset threshold, then a hit is declared. If this hit actually represents a true hit (i.e. the correct code phase has been determined), then the code has been officially acquired and the search comes to an end. If the hit is a false alarm, then the verification process cannot be consummated and the search must continue. In general the verification is characterized by an extended dwell time (e.g., $K\tau_d$, K>>1) assumed to be fixed and entering into the code tracking loop mode. Since a true hit corresponds to a single code, the time interval $K\tau_d$ sec can be regarded as the penalty time associated when a false alarm is declared. If the detector output falls below the preset threshold, then the local PN code generator steps to its next position and the search proceeds. Thus, at each test position, one of the two events can occur, namely, a false alarm, and indication that acquisition has occurred when the PN codes are

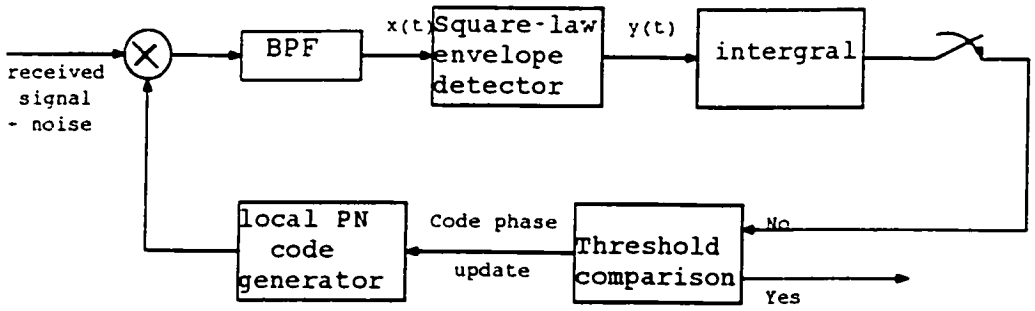

Figure 2.2: Block diagram of a single dwell PN acquisition system with non-coherent detection

actually misaligned, or no false alarm. The former event can occur with a probability of P_{fa} whereas the latter can occur with a probability of $(1\text{-}P_{fa})$, hence the Markov Chain model. Furthermore, at the true code phase position, either a correct detection can happen, i.e., an indication that acquisition has occurred when the PN code are indeed aligned, with probability P_d, or no detection occurs, with probability $(1\text{-}P_d)$. In the absence of any a-priori information regarding the true code phase position, the uncertainty in misalignment between the received PN code and the local replica code could be as much as a full code period. For long PN codes, the corresponding time uncertainty to be resolved could typically be quite large. In order to represent a reasonable compromise between the time required to search through this code phase uncertainty region and the accuracy within which the final alignment position is determined, the amount, which the local PN code generator is stepped in position as the search proceeds, must be judiciously chosen. It is typical in practice to require that the received and the local PN code signals be aligned to within one-half a code chip period $T_c/2$ before relinquishing control to the fine synchronization system (tracking loop). In accordance with this requirement, the time delay of the local PN code signal would be retarded (or advanced) in discrete steps of one half a chip period and a check for acquisition made after each step. If T_u represents the uncertainty time to be resolved, and we have

$$T_u = N_u T_c \tag{2.1}$$

then $q=2N_u$ would be the number of possible code alignments (these are referred to as cells) to be examined during each search through the uncertainty region.

The time to declare a true hit, T_{acq} (which is generally referred to as the Acquisition Time)[18], is a random variable and generally depends upon the initial code phase position of the local PN generator relative to that of the received code. The probability density function gives a complete statistical description of this random variable. The determination of the PDF would ultimately allow computation of the system. but one is often content with meansuring performance in terms of the first two moments of the PDF of T_{acq} namely the mean acquisition time $\overline{T_{acq}}$, and the acquisition time variance σ^2_{acq}.

2.2.1.2 Serial PN acquisition system: Single Dwell

In the following presentation of the performance of the acquisition time of a single dwell system, it will be assumed, for the sake of simplicity, that no code Doppler is present in the received signal and that the probability P_d is a constant (i.e., time invariant) which is equivalent to assuming that only one time corresponds to a "correct" code alignment. In the absence of a-priori knowledge concerning the relative code phase position of the received and locally generated codes, the local PN generator is assumed to start the search at any code phase position with equal probability. Stated mathematically, the probability P_1 of having the signal present (true hit) in the first cell searched is 1/q and the probability of not being present there is 1-1/q. For example, if the number of code chips to be searched is denoted by N_u and the search proceeds in half chip increments, then the number of cells to be searched is $q=2N_u$ and $P=1/2N_u$.

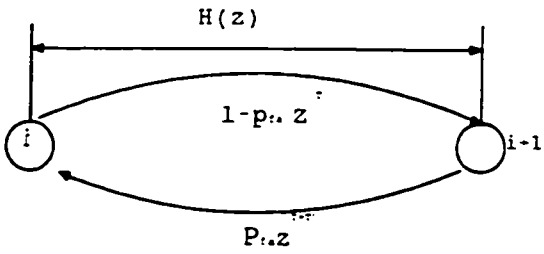

Figure 2.3: State-transition diagram of single-dwell system

Fig. 2.3 illustrates the generating function flow graph for the state-transition diagram which characterizes the acquisition process of the single dwell system. As is customary in such flow graphs, each branch is labeled with the product of the transition probability associated with going from the branch to the node at its terminating end, and an integer power of a parameter denoted by z. The parameter z is used to mark time as one proceeds through the graph and its power represents the number of time units (dwell times) spent in traversing that branch. Furthermore, the sum of the the branch probabilities (letting z=1) emanating from each node equals unity.

2.2.2 Serial PN acquisition system: Multiple-dwell

Fig.2.4 is the state-transition diagram of a typical multiple-dwell detector. Compared to Fig.2.3, it is much more complicated. We know that there is only one correct cell within the uncertainty region. Thus most of the cells evaluated by the energy detector are noise alone. An energy detection scheme that is capable of rejecting these incorrect phase cells rapidly while not letting P_{fa} become so large that false-alarm penalty time dominates synchronization time is desirable.

The multiple-dwell [19] detection scheme, discussed in this section, accomplishes this using multiple evaluations of the same phase cell. The first evaluation is very short and results in immediate rejection of many incorrect cells. The short integration time of this first evaluation also results in a high false-alarm probability.

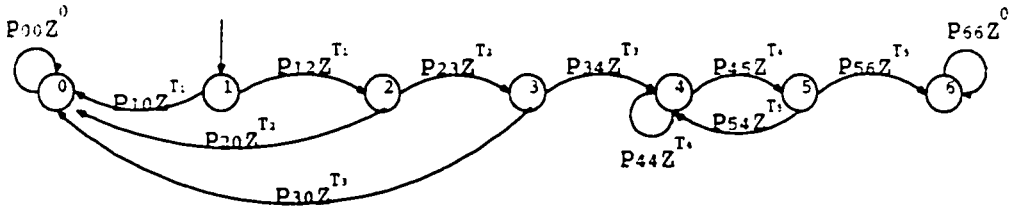

Figure 2.4: State-transition diagram of a typical multiple-dwell detector

When a false alarm occurs on the first evaluation, a second evaluation of the same cell begins, using a longer integration time. This second evaluation is capable of rejecting most of the false alarms of the first evaluation. The second evaluation may be followed by a third, fourth, or as many as desired to achieve a particular performance level. Since a particular phase cell may be rejected after one or more integrations, the time required to evaluate a cell is a random variable. All integration time thresholds as well as the logic followed by the multiple-dwell detection scheme are chosen to yield a minimum average synchronization time. Single-dwell is just a special case of the multiple-dwell systems.

Multiple-dwell techniques are a generalization of the single dwell serial PN acquisition with additional threshold testing that does not constrain the examination interval per cell to a constant interval of time. Nevertheless, this scheme falls into the class of fixed dwell time PN acquisition systems because of the fact that the variation in integration time is achieved here by allowing the examination interval to consist of a series of fixed short dwell periods (each generally longer than its predecessor) with a decision being made after each dwell. Allowing the integration time in a given cell examination interval to increase towards its maximum value in discrete steps, permits dismissal of an incorrect alignment earlier than would be possible in a single dwell system which is constrained to always integrate over the full examination interval. Since most of the cells searched correspond to incorrect alignments, the ability to quickly eliminate them produces a considerable reduction in acquisition time (particularly in the case of long codes).

Fig. 2.4 illustrates the N-dwell serial synchronization system with half chip search. The received signal plus noise is firstly multiplied by the local replica of the PN code and this is applied to each of N non-coherent detectors. The ith detector, i=1,2, ...N is characterized by a detection probability P_{Di}, a false alarm probability P_{fai}, and a dwell time τ_{di}. If it is assumed that the detector dwell times are ordered such that $\tau_{d1} \leq \tau_{d2} \leq ... \leq \tau_{dN}$ then the decision to continue or stop the search at the present cell is made by sequentially examining the N-detector outputs (starting with the first) and applying the following algorithm:

- If all the N detectors (tested in succession) indicate that the present cell is correct, i.e., each produces a threshold crossing, then the decision is made to stop the search.

- If any one detector fails to produce a threshold crossing (i.e., fails to indicate that the present cell is correct), then the decision is made to continue the search, the delay τ of the local PN generator is retarded by the chosen phase update increment, and the next cell is examined. Thus as soon as one detector indicates that the codes are misaligned, the search may move on without waiting for the decisions of the remaining detectors.

The power of the N-dwell system over the single dwell system lies in the fact that the maximum time to search a given cell is τ_{dN}, the minimum time is τ_{d1}, thus most of the cells can be dismissed after a dwell time τ_{dk}, k$\leq N$, whereas the single dwell system requires that each and every cell be examined for a time equivalent of τ_{dN}.

2.3 Matched Filter and Parallel Matched Filter

A highly efficient method of initial synchronization is to "matched filter" detect the received signal. The matched filter is designed to output a pulse when a particular sequence of code symbols is received. When this pulse is sensed, the receiver code

generator is started using an initial condition corresponding to the received code phase and synchronization is complete. This technique requires matched filters with extremely large time-bandwidth products. In the usual case where the spreading code period is long, the matched filter must also be easily programmable. For example, the spreading code period may be longer than the entire mission being carried out. Thus a matched filter designed for a single sequence of code symbols may never receive these symbols. A programmable matched filter can be programmed for a particular code phase which is dependent on an estimate of the propagations on high-speed digital correlators as well as programmable convolvers for this application.

In this method, each load is evaluated by attempting to despread the received signal just as was described for serial search techniques. This technique is called rapid acquisition by sequential estimation (RASE)[20]. A slightly modified version of this technique performs a preliminary evaluation to attempting the full correlation despreading evaluation. This modified technique is called recursion aided RASE (RARASE)[21].

Fig.2.5 is a top-level block diagram of a direct sequence spread-spectrum receiver which uses a matched filter synchronization processor. The received signal, including the desired signal and interference is input to the usual spreading code tracking loop and to the on-time despreader for data detection. In addition, the received signal is input to a bandpass filter, which is matched to a segment of the direct-sequence-spread waveform. When the waveform segment to which the filter is matched is received, the matched filter produces an output pulse. The synchronizer detects this pulse using an envelope detector followed by a threshold comparator. The spreading code generator is started at the correct phase when the matched filter output pulse is sensed. The started phase for the code generator is a function of the selected matched filter waveform segment and the matched filter and detection

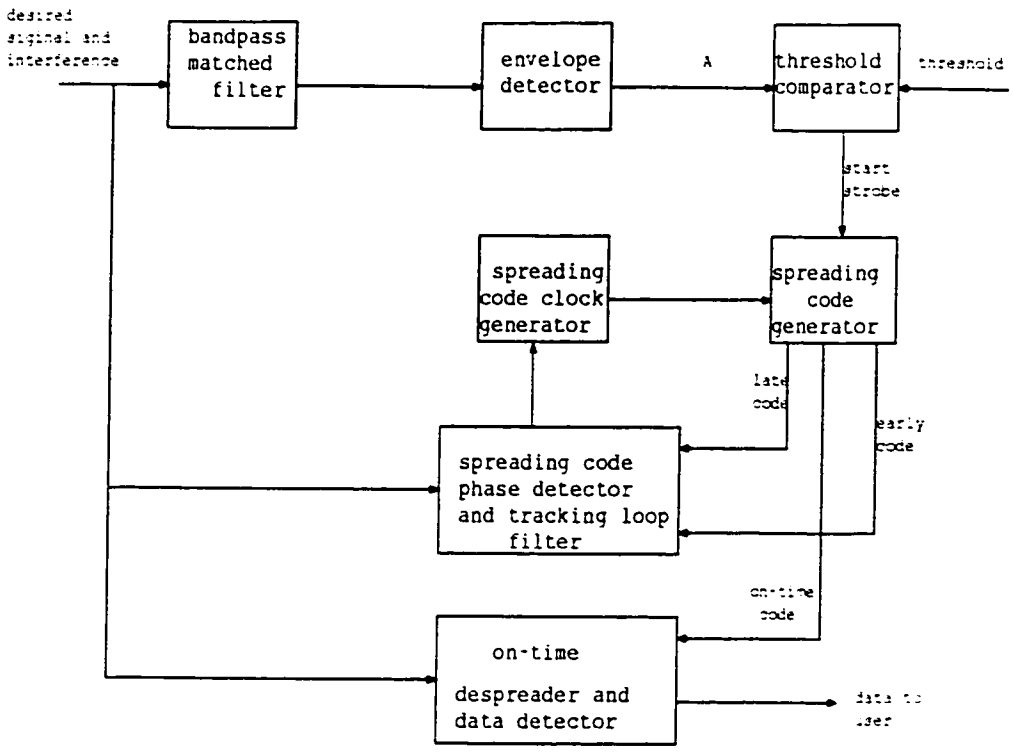

Figure 2.5: Direct-sequence spread-spectrum receiver using matched filter code acquisition

delays. The code generator starting phase is calculated prior to the start of the synchronization process and in some applications may be a constant set in the receiver design.

Based on the matched filter, it is the parallel matched filter. This is nothing but dividing the matched filter into several parts, each concentrating on one part of the phase, and these parallel parts are working separately and independently, and also each one outputs its own epoch time. Thus the acquisition time is shortened. It depends on how many parallel matched filter the system has. The more there is, the shorter the acquisition time.

2.4 Modified Sweep Strategies For Non-Uniform Distribution Signal

All the results up to this point have been derived by assuming that the received spreading waveform phase is uniformly distributed over a particular uncertainty region. Suppose now that the received phase distribution is defined by p(n)[22], the probability that the received phase is within the nth phase cell. When p(n) is known, the sweep strategy should be modified to search the most likely phase cells first and then the less likely cells. For example, if the received phase distribution were Gaussian, a reasonable search strategy would be to search the cells within one standard deviation of the most likely cell first and the expand the search to cells with two standard deviations, and so on. Note that p(n) is a discrete distribution and therefore cannot be Gaussian. The distribution of the received phase is however, continuous, the function p(n) is easily derived from the continuous density and the cell boundaries. Fig.2.6 illustrates the Gaussian distribution and the search strategy proposed by[23]. Observe that the received phase density has been truncated at three standard deviations.

The average synchronization time for the system is calculated using[24]:

$$\overline{T_s} = \sum_{n,j,k} Pr(n,j,k) \tag{2.2}$$

Where n,j, k are the particular location for the correct phase, the particular number of false alarms and the number of missed detections of the correct phase respectively. The proper limits for all summations for the three variables, j and k must be determined. If ΔT represents the time uncertainty region, Δt represents the phase step size, then $\frac{\Delta T}{\Delta t}$is an integer and represents the number of cells to be searched. The limits for the first summation are then $-\frac{C}{2} \leq n \leq \frac{C}{2}$[25] where cell

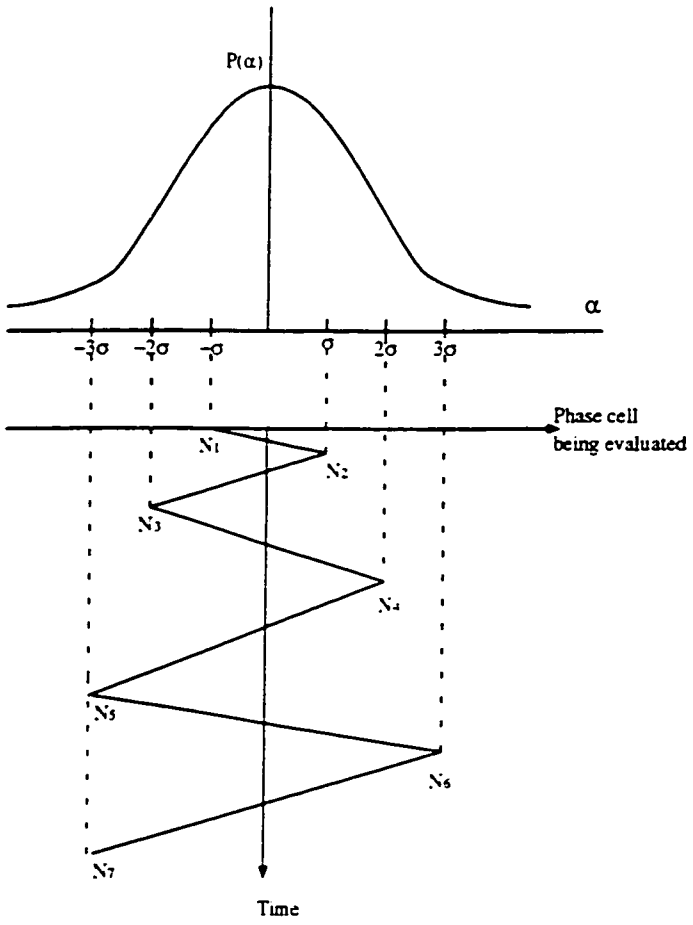

Figure 2.6: Received spreading waveform phase probability density and possible sweep strategy

number zero is at the center of the uncertainty region. The discrete probability of the n^{th} phase cell being correct is

$$p(n) = Aexp(-\frac{n^2}{2T^2}) \qquad -\frac{C}{2} \leq n \leq \frac{C}{2} \tag{2.3}$$

where A is a constant calculated from

$$\sum_{n=-\frac{C}{2}}^{\frac{C}{2}} p(n) = 1, \qquad T = \frac{C}{6} \tag{2.4}$$

Let each pass through the uncertainty region be numbered using the variable "b". Furthermore let N_b, and $N_{(b+1)}$ denote the starting and ending cell number for the bth pass. For the strategy of Fig.2.6, N_1=-C/6, $N_2 = C/6$, $N_3 = -C/3$, $N_4 = C/3$, and so on, where all fractions are rounded to the nearest intercells. Let f(n) denote the number of the pass that evaluated cell "n" for the first time. For example if C/6<n<C/3, the cell will not be evaluated until the third sweep. The limits of the sum over "j" are $0 \leq j \leq \infty$, the variable "k" is the total number of false alarms in all incorrect phase cells is denoted by K(n,j) and is given by

$$K(n,j) = \sum_{b=1}^{f(n)+j-1} |N_{b+1} - N_b| + |n - N_{f(n)+j}| - j \tag{2.5}$$

The false alarm can occur in any order within the K(n,j) incorrect phase cells and the number of false alarms is binomially distributed. Combining all of the above information yields

$$P(n,j,k) = A exp\left(-\frac{n^2}{2T^2}\right) P_d (1-P_d)^j \begin{pmatrix} K(n,j) \\ k \end{pmatrix} P_{fa}^k (1-P_{fa})^{K(n,j)-k} \tag{2.6}$$

and

$$\overline{T_s} = \sum_{n=-C/2}^{n=C/2} \sum_{j=0}^{\infty} \sum_{k=0}^{K(n,j)} \{[K(n,j)+j]T_i + kT_{fa}\} P(n,j,k) \tag{2.7}$$

The above equation has been evaluated in [26]. Modified sweep strategies have been used for many years in radar. Their use results in reduced average synchronization time when the distribution of the received phase is non-uniform.

Chapter 3

Simulation of Alternative Techniques For Code Acquisition In WCDMA Systems

3.1 Cell Search

Third Generation (3G) cellular systems are currently being standardized by various standardization bodies. One of the major differences between WCDMA and IS-2000 is that WCDMA supports asynchronous base stations, whereas IS-2000 relies on synchronized base stations. With synchronous base stations, all cells (or sectors) can use shifts of the same scrambling code, so that a call is identified by a unique code phase shift of the scrambling code. On the other hand, without time and frequency synchronization between base stations, using a different phase of the same code for scrambling is not sufficient to resolve the code ambiguity in the presence of time ambiguity. Thus in an asynchronous CDMA system, cells can only be identified by using distinct scrambling codes. WCDMA uses 512 downlink primary scrambling codes, allowing unique cell identification in every cluster of 512 cells. The process of searching for a cell and synchronizing to its downlink scrambling code is often

referred to as cell search. Cell search is necessary after the MS (mobile station) has switched on, and during idle and active modes, to identify new camping cell or hand over candidates, respectively. Idle and active mode search is also called target cell search. The performance of cell search impacts the perceived switch-on delay, stand-by time, and link quality, and thus is important to MS design.

In WCDMA, a cell is identified mainly by its downlink scrambling code. There are 512 primary downlink scrambling codes reused throughout the system. These 512 codes are based on length 2^{18} - 1 Gold code sequences truncated to one frame interval, which is 38400 chips for the chip rate of 3.84 Mchips/s. To reduce the complexity of searching through the 512 downlink primary scrambling codes, the concept of code grouping and the use of code group indicator codes (GIC)[27] were introduced. The scrambling code is identified by first identifying its code group to significantly reduce the degree of code uncertainty. The complexity of cell search is further reduced by combining code group identification and frame boundary synchronization into one stage. With this scheme, the time uncertainty is completely resolved when the code group identity is obtained. As a result, the complexity of identifying the scrambling code in the identified code group is significantly reduced. Schemes with further complexity reduction by increasing the number of code groups were proposed[1]. The 512 downlink primary scrambling codes are divided into 64 groups, each of 8 scrambling codes.

To facilitate cell search, three channels are used, namely the Primary Synchronization Channel (P-SCH)[28], the Secondary Synchronization Channel (S-SCH)[28], and the Common Pilot Channel (CPICH) [28]. The P-SCH together with the S-SCH are also referred as the Synchronization Channel (SCH). Fig.3.2 illustrates the slot and frame formats of these channels. Each frame of 38 400 chips (or 10 ms) is divided into 15 slots, of each 2560 chips (or 0.67 ms).

The CPICH, which is used to carry the downlink common pilot symbols, is scrambled by the primary downlink scrambling code of the cell. Within each CPICH

time slot, there are 10 pilot symbols, each spread by 256 chips. All symbols are QPSK modulated, and the modulation values of the pilot symbols are known once the MS knows the frame boundary. The spreading sequence of CPICH is taken from the set of Orthogonal Variable Spreading Factor (OVSF) codes [29], maintaining mutual orthogonality between CPICH and the other downlink channels also spread by OVSF codes, as show Fig. 3.1.

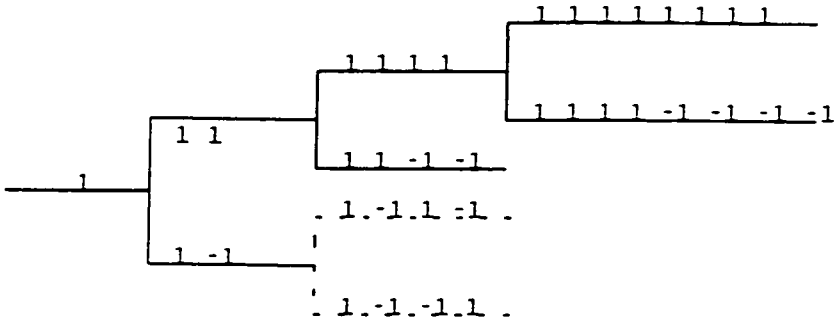

Figure 3.1: OVSF code

Unlike CPICH, neither the P-SCH nor the S-SCH is scrambled by the primary downlink scrambling code. Instead of the OVSF codes, other sequences of length 256 chips are used. The P-SCH sequence is transmitted once in the same position in every slot, and can thus be used for detecting the slot boundary. Furthermore, all cells use the same P-SCH sequence. As a result, only one P-SCH matched filter is needed to detect the slot boundaries of downlink signals.

The S-SCH is used to identify the frame boundary and scrambling code group identity. Unlike the P-SCH sequence, the S-SCH sequences vary from slot to slot. There are 16 S-SCH sequences, mapped correspondingly to 16 S-SCH symbols, labeled from 1 - 16. A frame (15 slots) of 15 such S-SCH symbols forms a codeword taken from a codebook of 64 codewords. The same codeword is repeated every frame in a cell. These 64 codewords correspond to the 64 code groups used throughout the system; thus a code group can be detected by identifying the codeword transmitted

in every S-SCH frame. Furthermore, the 64 codewords are all chosen to have distinct code phase shifts, and any phase shift of a codeword is different from all phase shifts of all other codewords. With these properties, the frame boundary can be detected by identifying the correct starting phase of the S-SCH symbol sequence. To maximize the minimum symbol distance of the codebook, between different cyclic shifts of the same codeword or between any cyclic shifts of different codewords, the use of a Comma-Free ReedSolomon (RS) code was proposed [22]. For 15 slots per frame, a (15, 3) ReedSolomon (RS) code over GF(16) is used. The RS code has a minimum distance of 13. Moreover, to minimize cross-channel interference, the 16 S-SCH sequences and the P-SCH are mutually orthogonal [30].

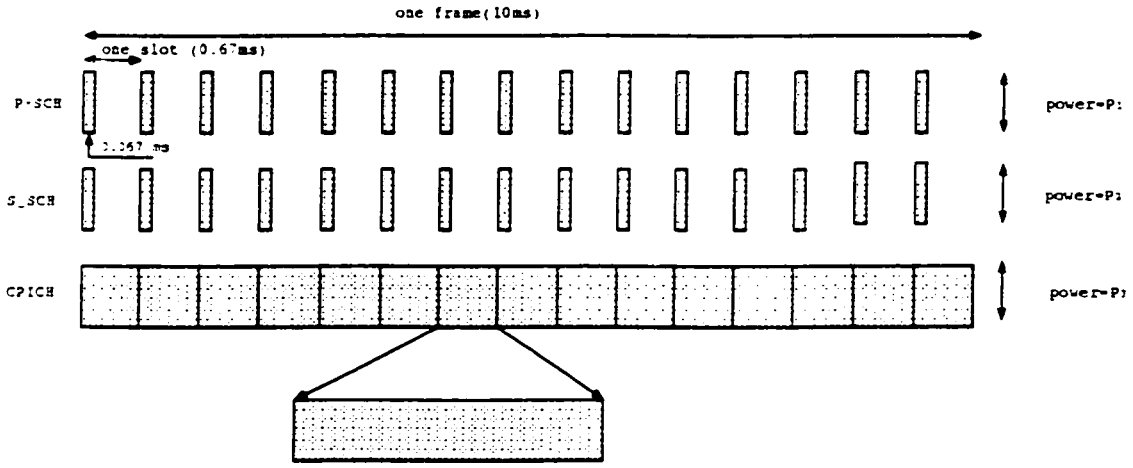

Figure 3.2: Frame and slot structures for CPICH, P-SCH, and S-SCH.

The cell search is typically carried out in three steps: slot synchronization; frame synchronization and code-group identification: and scrambling-code identification. An example procedure from [31] is described as follows:

Step 1: Slot synchronization. During the first step of the cell search procedure, the mobile station uses the SCH primary synchronization code to acquire slot synchronization to a cell. This can be done with a single matched filter matched to the primary synchronization code that is common to all cells. The slot timing of the cell can be obtained by detecting peaks in the matched filter output.

Step 2: Frame synchronization and code-group identification. During the second step of the cell search procedure, the mobile station uses the SCHs secondary synchronization code to find frame synchronization and identify the code group of the cell found in the first step. This is done by correlating the received signal with all possible secondary synchronization code sequences and identifying the maximum correlation value. Because the cyclic shifts of the sequences are unique, the code group and the frame synchronization are determined.

Step 3: Scrambling-code identification. During the third and last step of the cell search procedure, the mobile station determines the exact primary scrambling code used by the cell. The primary scrambling code is typically identified through symbol-by-symbol correlation over the CPICH with all codes within the code group identified in the second step. After the primary scrambling code has been identified, the primary P-SCH can be detected. And the system and cell specific information can be read.

In case the mobile station has received information about which scrambling codes to search for, steps 2 and 3 above can be simplified.

Given the above Synchronization Channels and CPICH, code and time synchronization can be achieved by the following stages: 1) slot boundary detection based on P-SCH (using a P-SCH matched filter); 2) frame boundary detection and scrambling code group identification based on S-SCH (using correlators, correlating against 16 S-SCH sequences, and an RS decoder); 3) scrambling code detection based on S-SCH (using correlators, correlating against all scrambling codes in the identified code group). For the initial search, the ultimate goal is to decode the cell identity of the acquired signal. To achieve this, two extra stages are needed: 4) frequency acquisition based on CPICH (to reduce initial frequency error so that the MS can decode the broadcast information); and 5) detecting cell identity (by reading the broadcast information). The frequency acquisition step is necessary because of the large frequency error after MS is powered on. Without correcting the

frequency error, the cell identity, transmitted is in the Broadcast Channel, cannot be decoded reliably. For the target cell search, there is no ambiguity in the mapping from a downlink scrambling codes and the cell identity of a neighboring cell. Thus, identifying (and synchronizing to) the downlink scrambling code is sufficient to identify any given cell of interest. So in this thesis, we will only consider stage1, stage2 and stage3 of the acquisition process as in Fig. 3.3.

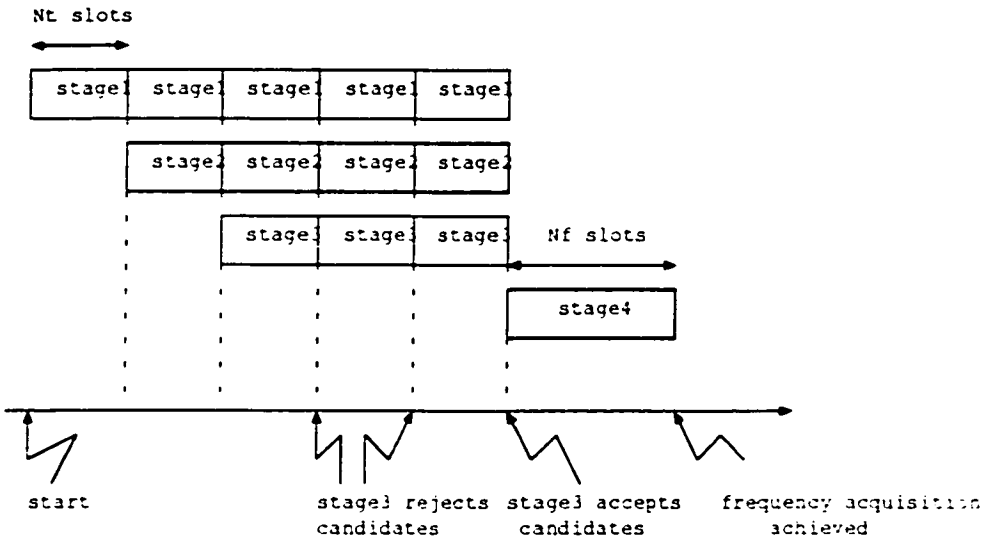

Figure 3.3: cell search procedure

We will focus on the code, time, and frequency acquisition aspects of cell search. Hence, stage 5 will not be addressed. Pipelined processing for stages 1, 2, and 3 is considered, as illustrated in Fig. 3.3. Stage 4 frequency acquisition is only activated when time and code synchronization is achieved. To minimize the delay in the pipe (no idle time in the pipe)[32], the synchronization times used in stages 1, 2, and 3 are the same (N_t slot). According to Fig 3.3, stage1 always generates a list of slot boundary candidates at the end of each cycle. Based on each of the slot boundaries detected in stage 1, stage2 finds S-SCH and performs S-SCH correlations and RS decoding . At the end of each detection cycle, stage 2 always gives a list of candidates of frame boundary-code group pair to stage 3 for identification of the

scrambling code. In contrast to stage 1 and 2, stage 3 only activates stage 4, when a candidate is detected with high confidence. The acquisition time for code and time synchronization is of interest. According to Fig. 3.3 the acquisition time can be defined as the time interval between the time when stage 3 terminates the process. If stage 3 went through K3 cycles before it accepts a detected code and terminates the pipelined process, the acquisition time is given by :

$$T_{acq} = (K_3 + 2)N_t T_{slot} \tag{3.1}$$

We produce a 255 period Gold Code which is used by P-SCH and S-SCH. Since N=255, n=8. One is the entry octal notation $(551)_8$ in the primary polynomials[33] which may be used to generate an m-sequence of length 255. Gold Code 255 is used by the Primary Synchronization Channel and the Second Synchronization Channel. Another is the entry octal notation $(703)_8$. This preferred pair of m-sequences have period $N = 2^n - 1$. A typical shift register configuration used to generate a family of Gold codes is illustrated in Fig.3.5. The complete family of Gold codes for this generator is obtained using different initial loads of either of the shift registers.

$$g_1(D) = 1 + D + D^6 + D^7 + D^8 \tag{3.2}$$

$$g_2(D) = 1 + D^3 + D^5 + D^6 + D^8 \tag{3.3}$$

It follows as in Fig 3.4:

In WCDMA, a cell is identified mainly by its downlink scrambling code. There are 512 primary downlink scrambling codes reused throughout a system. These 512 codes are based on length $2^{18} - 1$ Gold sequences:

$$g_1(D) = 1 + D + D^7 + D^{18} \tag{3.4}$$

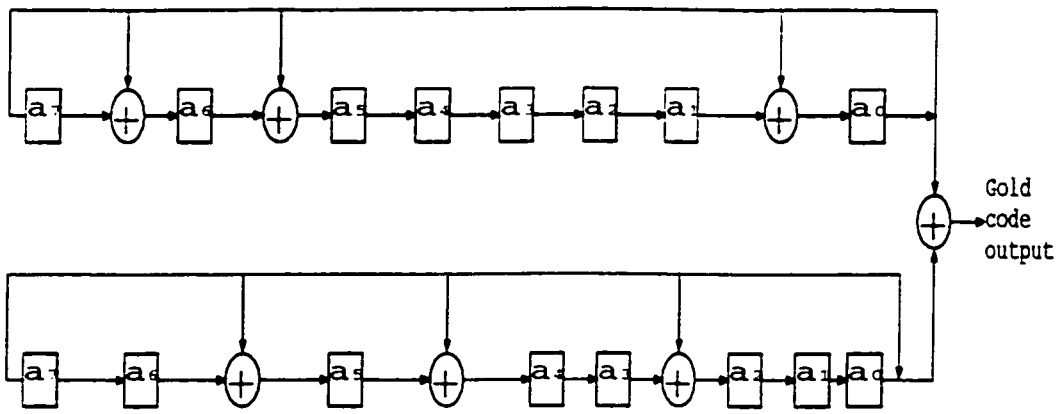

Figure 3.4: 255 Gold code register

$$g_2(D) = 1 + D^5 + D^8 + D^{10} + D^{18} \tag{3.5}$$

truncated to one frame interval, which is 38 400 chips for the chip rate 3.84 Mchips/s. To reduce the complexity of searching through the 512 downlink primary scrambling codes, we use the concept of code grouping and the use of code group . The scrambling code is identified by first identifying its code group to significantly reduce the degree of code uncertainty. The complexity of cell search is further reduced by combining code group identification and frame boundary synchronization into one stage . With this scheme, the time uncertainty is completely resolved when the code group identity is obtained. As a result, the complexity of identifying the scrambling code in the identified code group is significantly reduced. There are schemes with further complexity reduction by increasing the number of code groups . The 512 downlink primary scrambling codes are divided into 64 groups, each of 8 codes.

3.2 Our simulation model

In this section, we describe acquisition system and signal models. The desired signal s(t) is scaled with power P and the Gaussian noise n(t) is scaled by power Px. Hence, the signal-to-noise ratio (SNR) is given by P/Px. For stages 1 and 2, the desired

signal is the Synchronization Channel (P-SCH–S-SCH); whereas for stages 3 and 4, the desired signal is CPICH. Our channel model is shown in Fig. 3.5.

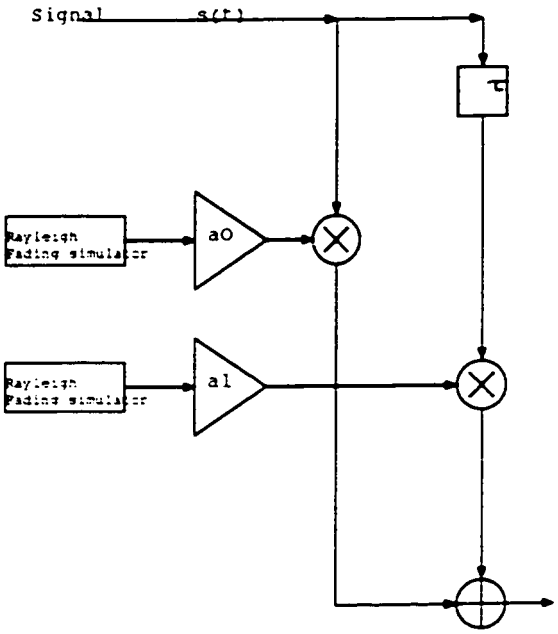

Figure 3.5: Channel model

A system model which includes the SCH and CPICH signals as illustrated in Fig 3.6 is used. Signals $s_1(t)$, $s_2(t)$ and $s_3(t)$ represent the normalized P-SCH, S-SCH, and CPICH signals, respectively. Noise $n_1(t)$ is used to model the intra-cell interference, $n_2(t)$ is used to model the inter-cell interference.

The desired signal in flat fading channel is simulated as:

$$r(t) = a_0 s(t) + a_1 s(t) + n(t) \tag{3.6}$$

The desired signal in frequency selective fading channel is given by:

$$r(t) = a_0 s(t) + a_1 s(t+\tau) + n(t) \tag{3.7}$$

Where a_0, a_1 are Raleigh distributed random variables with variance σ_r^2 . $r(t)$ is the code signal to be acquired, $n(t)$ is AWGN of power $N_0/2$ which includes both intra and intercell interference.

Throughout this thesis, the P-SCH sequence is represented by $(C_0^{(0)}, C_1^{(0)}, .., C_{255}^{(0)})$, and the mth S-SCH sequence is denoted by $(C_0^{(m)}, C_1^{(m)}, .. , C_{255}^{(m)})$, m = 1, 2, .. , 16, where $C_l^{(m)} \in \{1, -1\}$, l =0, 1, ... ,255, m = 0,1, .. , 16, are the chip values.

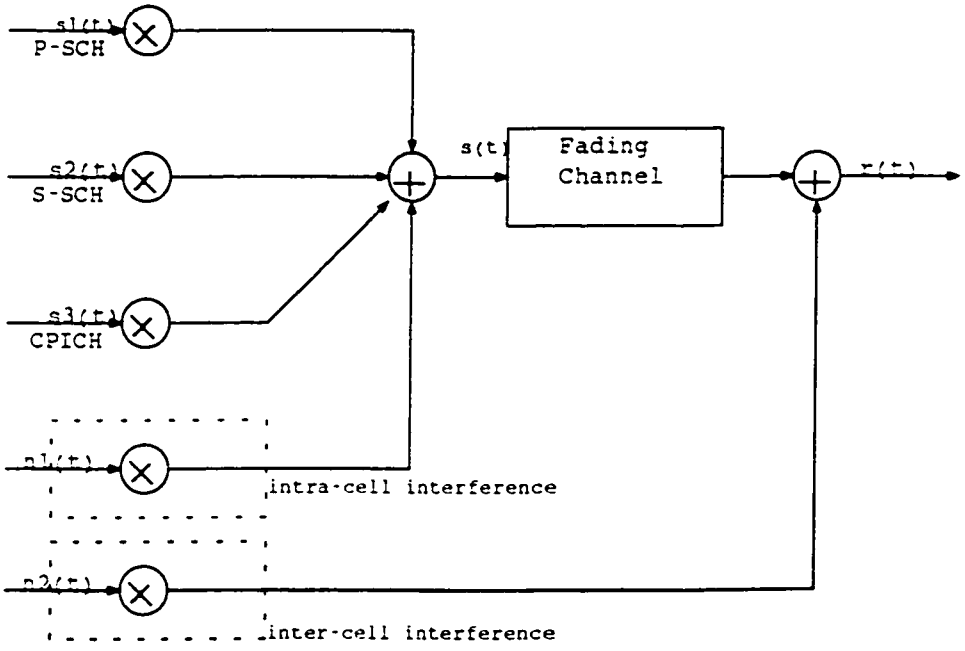

Figure 3.6: Signal model

A. Stage 1: Slot Synchronization

In stage 1, the P-SCH matched filter is used to detect the slot boundary. Due to a low operating signal-to-noise ratio, the matched filter outputs have to be noncoherently accumulated over many slots to get reliable decision statistics. After accumulation, a number of candidates are identified as possible slot boundary candidates. In our study, we use one sample per chip for r_k, and optimum sampling timing.

The matched filter output in our simulation program is given by:

$$y_k = \sum_{i=0}^{255} r_{k-i} c_{255}^{(0)} \tag{3.8}$$

The match filter output according to this architecture is given by using non-coherent combining:

$$y_k = \sum_{i=0}^{k-1} \left| y_k^{(i)} \right| \tag{3.9}$$

$$y_k^{(i)} = \sum_{l=0}^{M-1} r_{k-iM-l} c_{255-iM-l}^{(0)} \tag{3.10}$$

where M is the length of each short sequence, and K is the number of short sequences such that KM=256 . The length of each short sequence M, determines the performance of slot synchronization in the presence of frequency error. A larger M results in more phase rotation during matched filtering and larger incoherence loss. However, a large M also results in better noise suppression and may thus improve performance. So we selected M = 256.

A sample of our simulation results for the first acquisition stage in different fading environments is shown in Fig 3.7, where synchronization error rate is shown. The number of failed decision trials are the total number of short codes generated per simulation.

The performance of stage 1 with 15 slots (10 ms) in flat fading channels is shown in Fig. 3.7

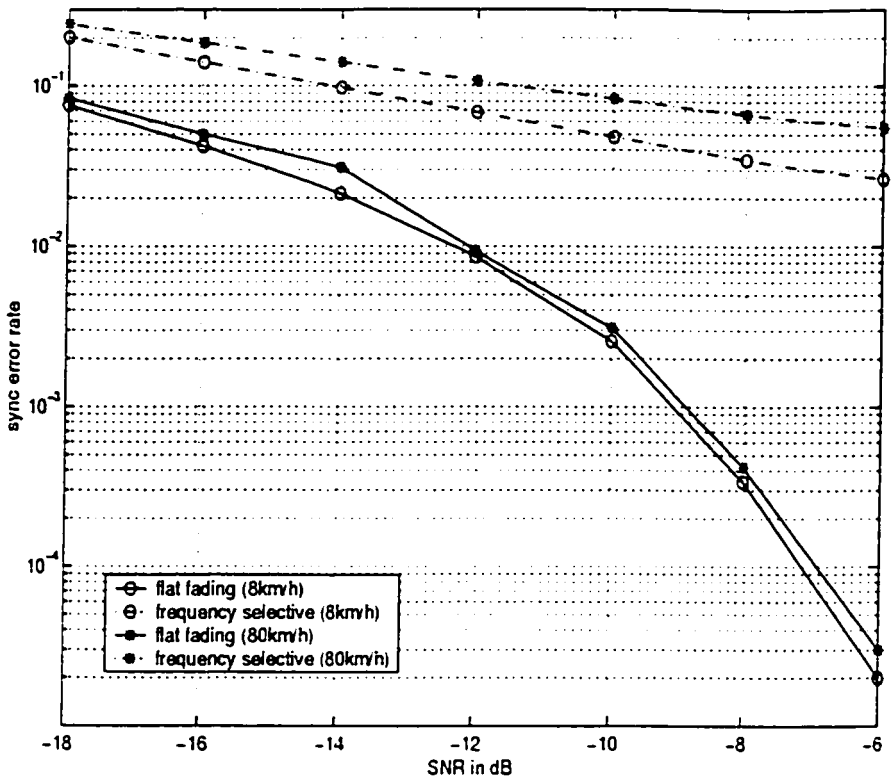

Figure 3.7: Stage 1 P-SCH Acquisition Performance .

B. Stage 2: Frame Synchronization and Code Group Identification

i) After achieving slot synchronization, S-SCH can be easily achieved. In stage 2, the receiver of the simulation program of operations starts by correlating the received signal of SCH with all 16 S-SCH sequences, and then accumulates S-SCH correlations over Nt slots according to the 64 RS codewords used; a (15, 3) ReedSolomon (RS) code over GF(16) [34] is used. The RS code has a minimum distance of 13. Moreover, to minimize cross-channel interference, the 16 S-SCH sequences and the P-SCH are mutually orthogonal [35], each with 15 hypothesized frame boundaries. The total number of hypotheses is therefore 960 (64 codewords times 15 shifts). A sample of our simulation results for the second acquisition stage in different fading environments is shown in Fig 3.8, where synchronization error rate is shown.

For received slot k, the simulation calculates S-SCH correlations as:

$$S_m(k) = \left| \sum_{j=0}^{255} r_j^{(k)} c_j^{(m)} \right| \tag{3.11}$$

m=1,2,3,...,16, k=0,1,...,Nt-1

ii) Accumulate S-SCH correlation values. Since the RS codewords are periodically repeated in every frame, if Nt >15, the correlation values corresponding to the same S-SCH sequence in different frames can be combined:

$$S'_m(k) = \sum_{j=0}^{N_t-1} S_m(j) \tag{3.12}$$

m =1, ... , 16, k=0, ... ,14.

iii) RS code decoding. For this step, the simulation program uses table decoding[30].

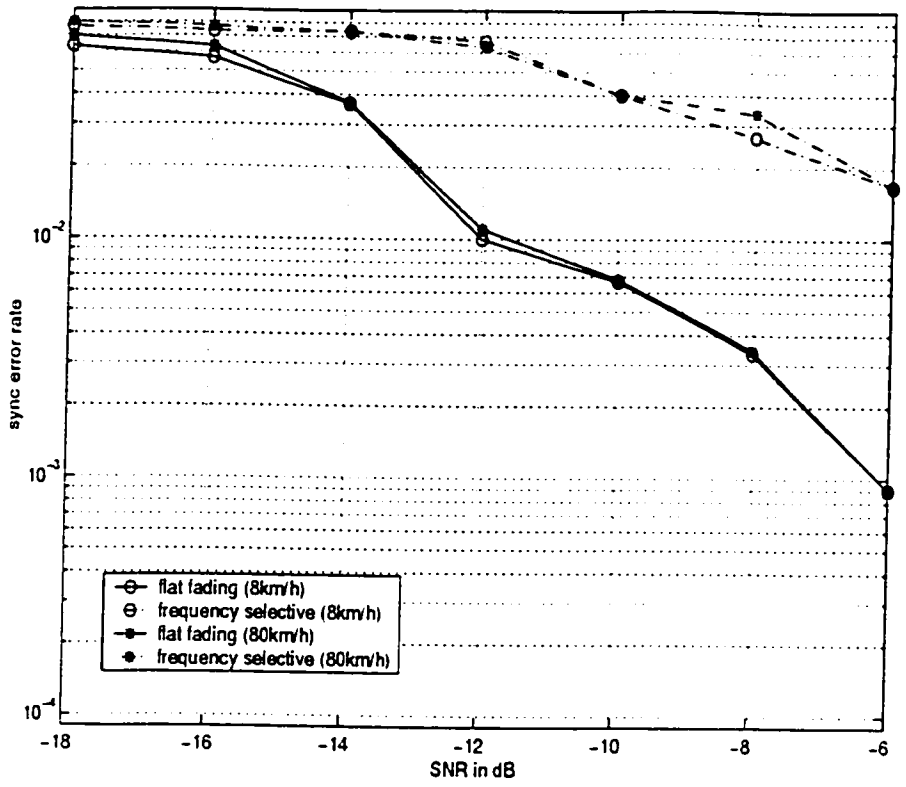

Figure 3.8: Stage 2 S-SCH Acquisition Performance

C. Stage 3: Scrambling Code Identification

After identifying the scrambling code group and achieving code synchronization, the downlink primary scrambling code can be identified by correlating the CPICH with all possible scrambling codes in the identified code group in our simulation program. The number of scrambling codes in the identified code group, N_{lc} =8, whereas for idle and active mode search, N_{lc} is typically 1 or 2, given a good system-wide code planning. One of the main design considerations in this stage is the probability of false detection. According to Fig. 3.9, stage 3 accepts a candidate only when the detection metric is greater than a threshold, where the threshold is predetermined to achieve a certain false detection probability.

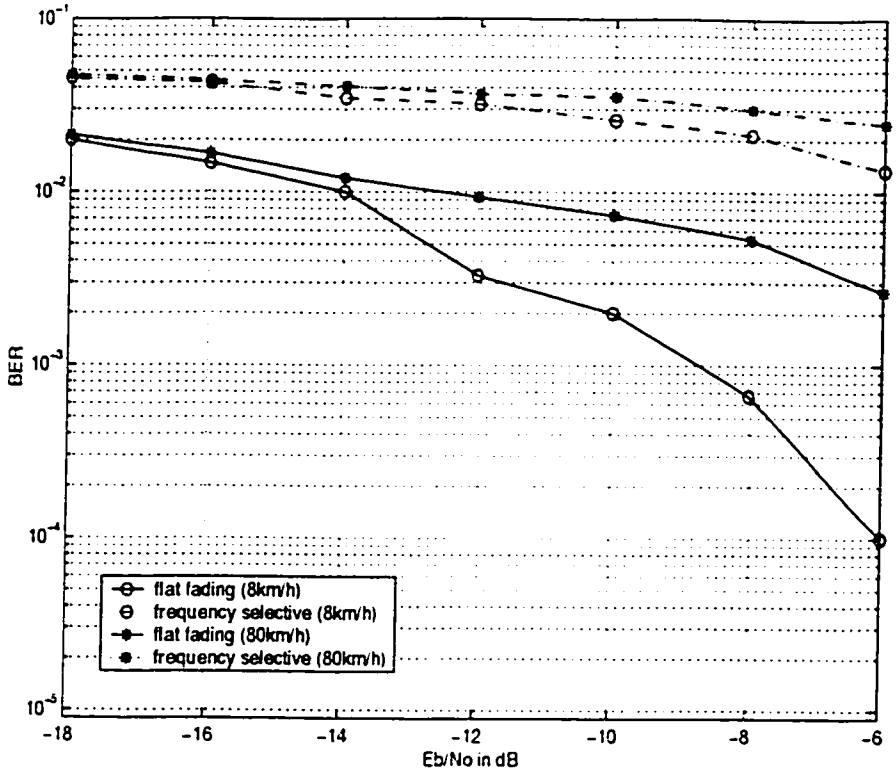

Figure 3.9: Stage 3 CPICH Acquisition Performance

We show some different thresholds and different probabilities of false alarm. The probability of detection is the integral from V_t to infinity of the envelope detector output pdf evaluated for the maximum signal-to-noise ratio. Probability of false alarm is the same integral evaluated at the minimum signal-to-noise ratio. These calculations are depicted in Table 3.1, which shows the V_t and P_d . Both P_d and P_{fa} are functions of SNR and V_t and cannot be independently selected. For a specific SNR, the selection of P_{fa} implies a particular threshold V_t which then sets P_d . Threshold values for P-SCH acquisition in flat fading channel (G=0) is follow in Table 3.1. Similar results for CPICH in flat fading channel (G=0) are shown in Table 3.2. G means the ratio between the power of total three channels plus intra-cell interference and the power of inter-cell inter-cell interference.

In our simulation,we use six policies to get better acquisition time. The six

Table 3.1: Threshold V_{t2} and P_{fa2} in P-SCH.

V_{t2}	15	18	21	24	27	30	33
P_{fa2}	6×10^{-3}	2×10^{-3}	6.3×10^{-4}	1×10^{-4}	4×10^{-5}	1×10^{-5}	10^{-6}
P_{d2}	0.9812	0.9724	0.9640	0.9568	0.9379	0.9047	0.8959

Table 3.2: Threshold V_{t3} and P_{fa3} in CPICH.

V_{t3}	81	99	116	130	144	157	172
P_{fa3}	6.5×10^{-3}	3×10^{-3}	7×10^{-4}	2×10^{-4}	6×10^{-5}	10^{-5}	10^{-6}
P_{d3}	0.9992	0.9918	0.9859	0.9746	0.9532	0.9350	0.9180

policies are based on certain utilization of serial, matched filtering and pipeline operations. We will show all acquisition times in flat fading channels and frequency selective fading channel. We want to show the average time in realistic channel conditions; two cases in flat fading channel-CASE I (Vehicular, 8km/h), CASE II (Vehicular, 80 km/h).We use six Policies to acquire code synchronization. The main contribution of this research is the utilization in Policy6. Different options of pipeline and serial search form the overall acquisition process from stage to stage. There are:

First Policy In Fig 3.10, uniformly distributed random variable y is called, If the output of this U(0,1) lies in the range [0 1/125], this means the search code phase is the correct one and so the simulation program proceeds to branch A in Fig 3.10, if the output of U(0,1) lies outside the range [1, 1/125], the simulation program continues to branch B which then adds T_1, T_2 and T_3 to the failed acquisition trials and the flow chart gets finally to branch C, where U(1,0) is called again. Similarly continuing from branch A, U(0,1) is called and T_1, T_2 and T_3 are added to the acquisition time counter.In other papers, they all choose T_1,T_2 and T_3 from 10ms to 30 ms. So we follow them. In our research we choose T_1=10ms, T_2= 20ms and T_3=30ms.

In Fig 3.10, P_{m1} means the probability of missing detection in stage1. This is calculated from a separate simulation routine where we transmit the P-SCH code.

P_{m1} is how many times we cannot get this code by using matched filter, even if the arriving code phase matches with the local matched filter phase .

In Fig 3.10, P_{m2} means the probability of missing detection in stage2. This is calculated from a separate simulation routine where we transmit S-SCH code. P_{m2} is how many times we can not get this code by using maximum-selection method (no thresholds set over correlators outputs).The correlation is performed with 256 chips.

In Fig 3.10, P_{m3} means probability of missing detection in stage3. This is calculated from a separate simulation routine where we transmit CPICH code. P_{m3} is how many times we cannot get this code by using the maximum-selection method (no thresholds set over correlators outputs).The correlation is performed with 2560 chips.

In Fig 3.10, P_f means probability of false alarm detection in stage1. This is calculated from a separate simulation routine where we transmit only AWGN (no code transmitted), and we get the highest peak which does not match the phase of the desired code.

In Fig 3.10, P_{e1} means probability of false alarm detection in stage2. This is calculated from a separate simulation routine where we transmit S-SCH code which is not the desired signal. P_{e1} is how many times we can get this code by using maximum-selection method(no thresholds set over correlators outputs). The correlation is performed with 256 chips.

In Fig 3.10, P_{e2} means the probability of false alarm detection in stage3. This is calculated from a separate simulation routine where we transmit CPICH code which is not the desired code, P_{e2} is how many times we can get this code by using maximum-selection method. The correlation is performed with 2560 chips.

We attempt to go to the first stage. If acquisition fails, we go back to the beginning. If $y < 1\text{-}P_m$, where y is a uniformly distributed random variable between (0,1), we will go to the second stage. In the second stage, if acquisition fails (in Fig

3.10 this means $y>1-P_{m2}$) the program does not go to stage 3, it returns to start. Only if we get the second code, we will go to the third stage. In the third stage, if acquisition fails (in Fig 3.10. this means $y>1-P_{m3}$) and so the program does not go to stage 4, we return start. We calculate acquisition time at every stage. We assume the first stage acquisition time $T_1 = 10ms[36]$,the second stage acquisition time $T_2 = 20ms[36]$, and the third stage acquisition time $T_3 = 30ms[1][36]$.

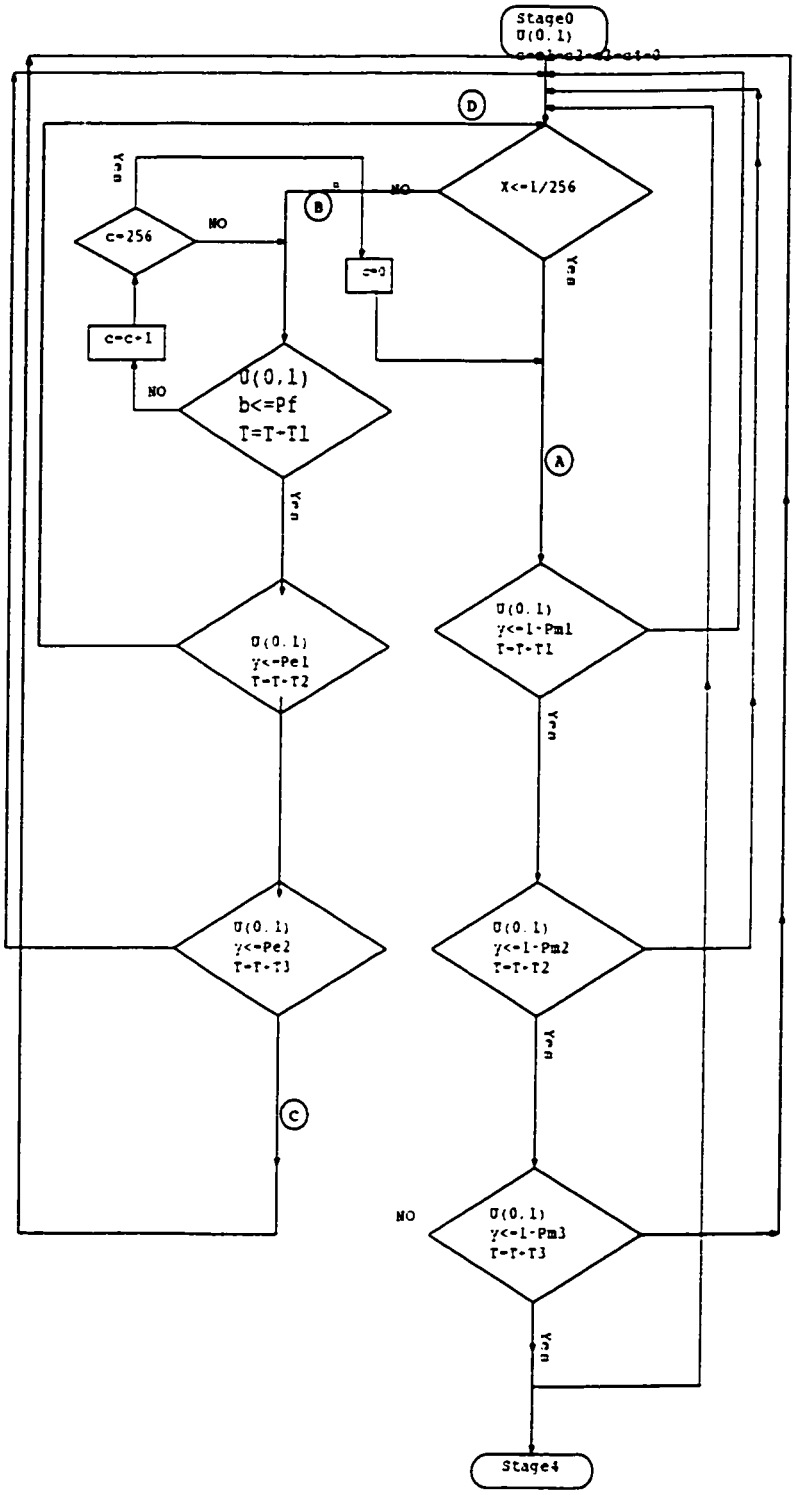

Figure 3.10: Flow chart of Policy 1

Second Policy In Fig 3.11, uniformly distributed random variable y is called if the output of this U(0,1) lies in the range [0 1/125], this means the search code phase is the correct one and so the simulation program proceeds to branch A in Fig 3.11, If the output of U(0,1) lies outside the range [1, 1/125] the simulation program continues to branch B which then adds T_1, T_2 and T_3 to the failed acquisition trials and the flow chart gets finally to branch C, where U(1,0) is called again. Similarly continuing from branch A, U(0,1) is called and T_1, T_2 and $T_3$are added to the acquisition time counter.

In Fig 3.11, P_{th1} means the probability of missing detection in stage1. This is calculated from a separate simulation routine where we transmit P-SCH code. P_{th1} is how many times we cannot get this code by using match filter.

In Fig 3.11, P_{th2} means the probability of missing detection in stage2. This is calculated from a separate simulation routine where we transmit S-SCH code. P_{th2} is how many times we can not get this code by the using the maximum-selection method and the fixed threshold .The correlation is performed with 256 chips.

In Fig 3.11, P_{th3} means the probability of missing detection in stage3. This is calculated from a separate simulation routine where we transmit CPICH code. P_{th3} is how many times we can not get this code by using the maximum-selection method and the fixed threshold.The correlation is performed with 2560 chips.

In Fig 3.11, P_f means the probability of false alarm detection in stage1. This is calculated from a separate simulation routine where we transmit only AWGN, and we get the highest peak which is not the desired signal.

In Fig 3.11, P_{e1} means the probability of false alarm detection in stage2. This is calculated from a separate simulation routine where we transmit S-SCH code which is not the desired signal, P_{e1} is how many times we can get this code by using the maximum-selection method and the fixed threshold. The correlation is performed with 256 chips.

In Fig 3.11, P_{e2} means the probability of false alarm detection in stage3.This is

calculated from a separate simulation routine where we transmit CPICH code which is not the desired signal, P_{e2} is how many times we can get this code by using the maximum-selection method and the fixed threshold. The correlation is performed with 2560 chips.

We attempt to go to the first stage .If acquisition fails it means y>1-P_{th1},where y is a uniformly distributed random variable between (0,1), we go to start. Only if we get the first code, we will go to the second stage. In the second stage,we use maximum-selection method and fixed threshold .If acquisition fails it means y>1-P_{th2}, we go back to start. Only if we get the second code, we will go to the third stage. In the third stage, we use maximum-selection method and fixed threshold. If acquisition fails it means y>1-P_{th3} , we go to start.We calculate acquisition time every stage. We assume $T_1 = 10ms$[36] , $T_2 = 20ms$[36], and $T_3 = 30ms$[36].

The difference between Policy 1 and Policy 2 is that we use a fixed threshold in stage2 and stage 3.

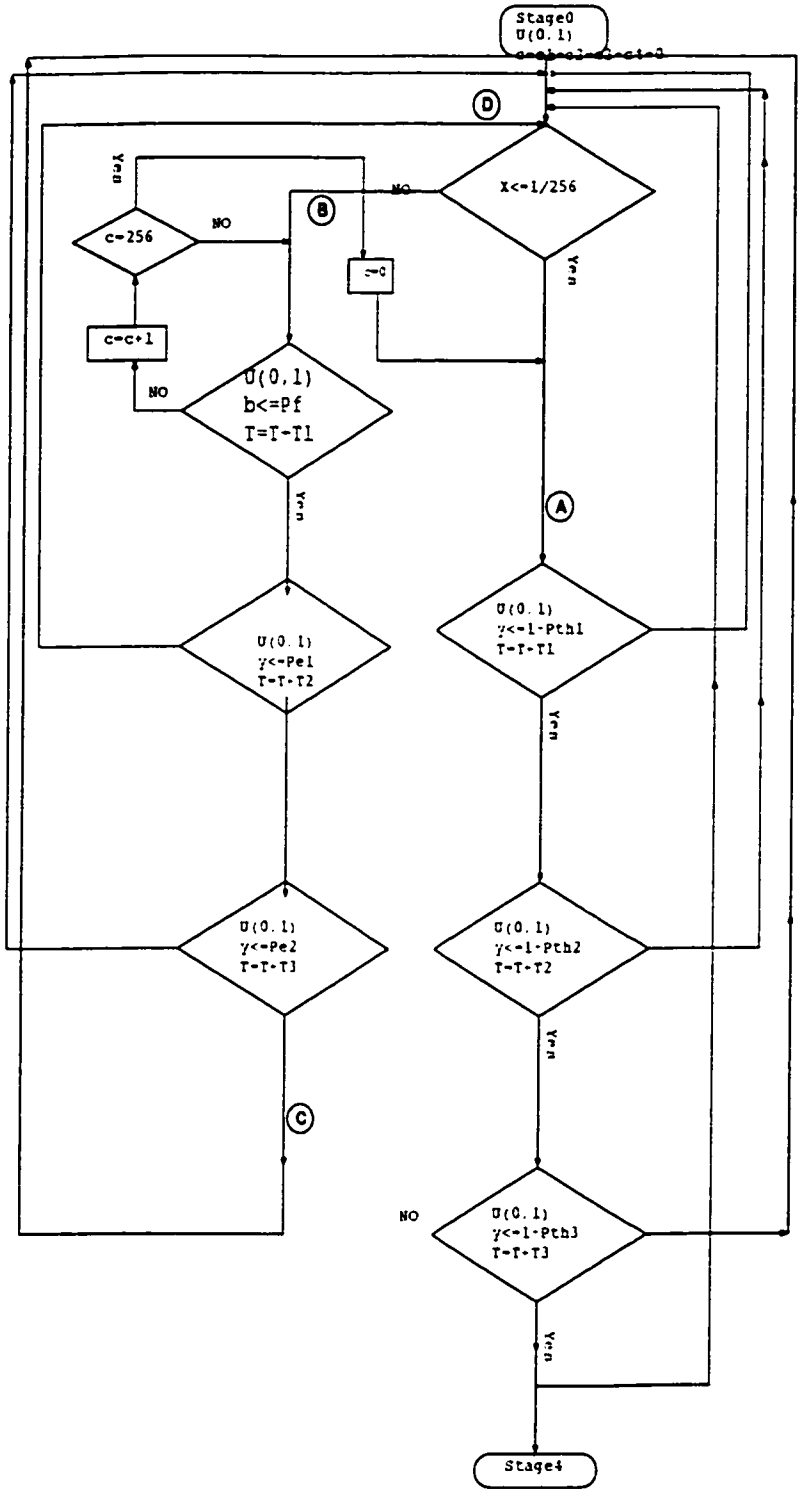

Figure 3.11: Flow Chart of Policy 2

Third Policy In Fig 3.12, uniformly distributed random variable y is called means if the output of this U(0,1) lies in the range [0 1/125], then the search code phase is the correct one and so the simulation program proceeds to branch A in Fig 3.12, in other case after it fails in stage2 not more than three times, it continues to branch A. If the output of U(0,1) lies outside the range [1, 1/125],the simulation program continues to branch B which then adds T_1, T_2 and T_3 to the failed acquisition trials and the flow chart gets finally to branch C and if it fails the simulation program proceeds to branch E in Fig3.12 not more than three times. then we try u(1,0) is called again. Similarly continuing from branch A, U(0,1) are called and T_1, T_2 and $T_3$are added to the acquisition time counter.

In Fig 3.12, P_{th1} means the probability of missing detection in stage1. This is calculated from a separate simulation routine where we transmit P-SCH code. P_{th1} is how many times we can not get this code by using match filter.

In Fig 3.12, P_{th2} means the probability of missing detection in stage2. This is calculated from a separate simulation routine where we transmit S-SCH code. P_{th2} is how many times we can not get this code by using the maximum-selection method and the fixed threshold .The correlation is performed with 256 chips.

In Fig 3.12 P_{th3} means the probability of missing detection in stage3. This is calculated from a separate simulation routine where we transmit CPICH code. P_{th3} is how many times we can not get this code by using the maximum-selection method and the fixed threshold .The correlation is performed with 2560 chips.

In Fig 3.12, P_f means the probability of false alarm detection in stage1. This is calculated from a separate simulation routine where we only transmit AWGN, and we get the highest peak which is not the desired signal.

In Fig 3.12, P_{e1} means the probability of false alarm detection in stage2. This is calculated from a separate simulation routine where we transmit S-SCH code which is not the desired signal, P_{e1} is how many times we can get this code by using the maximum-selection method and the fixed threshold. The correlation is performed

with 256 chips.

In the Fig 3.12 P_{e2} means the probability of false alarm detection in stage3.This is calculated from a separate simulation routine where we transmit CPICH code which is not the desired signal, P_{e2} is how many times we can get this code by using the maximum-selection method and the fixed threshold. The correlation is performed with 2560 chips.

We attempt to go to the first stage only if we get the first code. Thatis if $y<1-P_{th1}$,where y is a uniformly distributed random variable between (0,1) ,we will go to the second stage. In the second stage,we use maximum-selection method and fixed threshold . If acquisition fails it means $y>1-P_{th2}$, we will go to stage1 again and try three times. If acquisition fails, we go to start. Only if we get the second code, we will go to the third stage. In the third stage, we use maximum-selection method and fixed threshold . If acquisition fails it means $y>1-P_{th3}$, we go to stage2 again and try three times. If acquisition fails, we go back to start. We calculate acquisition time every stage. We assume $T_1 = 10ms$[36] , $T_2 = 20ms$[36], and $T_3 = 30ms$[36].

The difference between Policy 3 and Policy 2 is that we go back to branch A if y is larger than 1 - P_{th2} and we return to branch E if y is larger than 1 - P_{th3} . In Policy 2 and Policy 1, we go back to start if the condition is not satisfied.

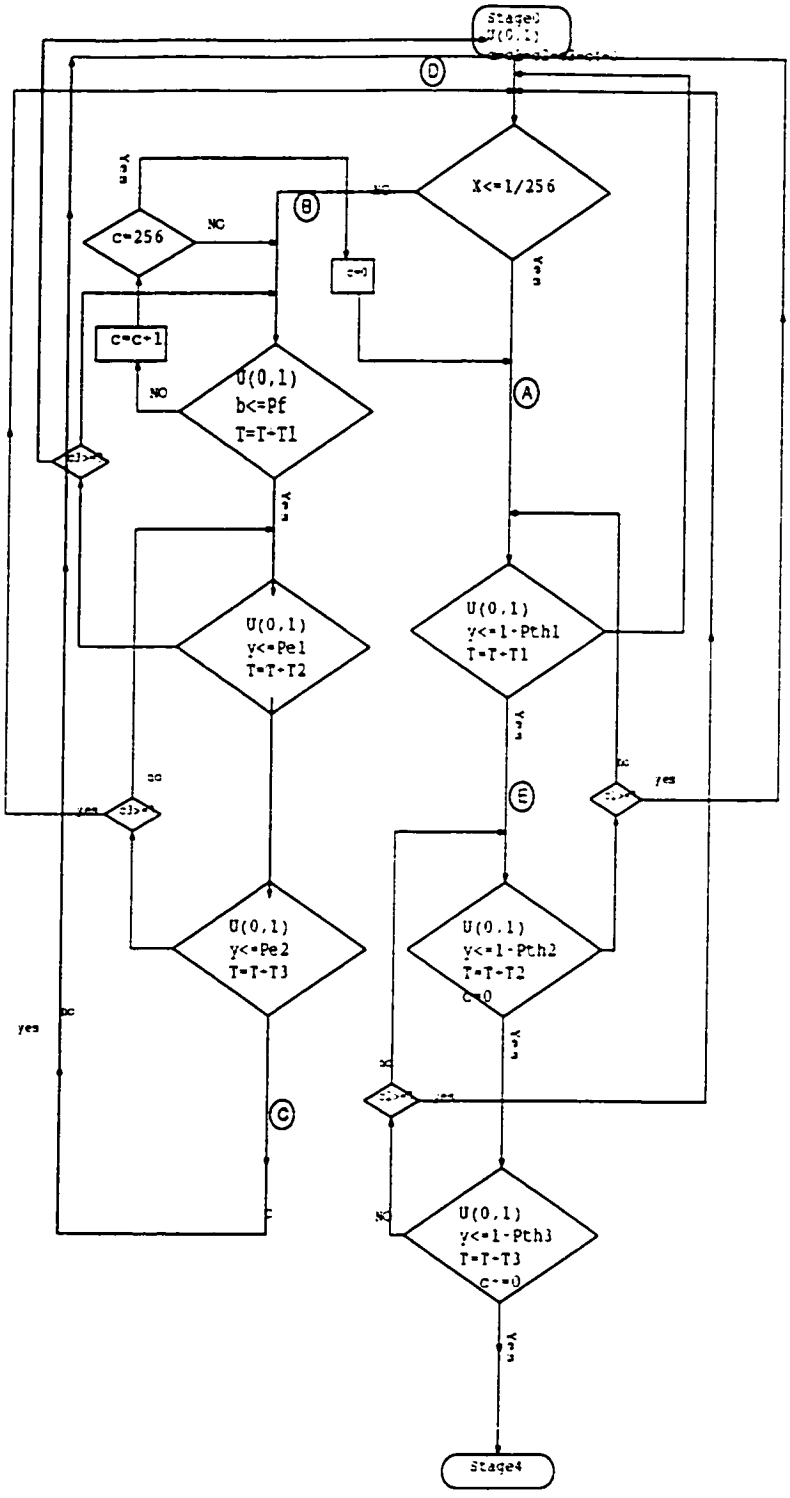

Figure 3.12: Flow Chart of Policy 3

Fourth Policy In Fig 3.13, uniformly distributed random variable y is called. If the output of this U(0,1) lies in the range [0 1/125], this means the search code phase is the correct one and so the simulation program proceeds to branch A, in other case after it fails in stage2 or stage3 not more than three times, it continue to branch A, if the output of U(0,1) lies outside the range [1, 1/125], the simulation program continues to branch B which then adds T_1, T_2 and T_3 to the failed acquisition trials and the flow chart gets finally to branch C, and where U(1,0) is called again. Similarly continuing from branch A, U(0,1) are called and T_1, T_2 and T_3 are added to the acquisition time counter.

In Fig 3.13, P_{th1} means the probability of missing detection in stage1. This is calculated from a separate simulation routine where we transmit P-SCH code , P_{th1} is how many times we can not get this code by using match filter.

In Fig 3.13, P_{th2} means the probability of missing detection in stage2. This is calculated from a separate simulation routine where we transmit S-SCH code. P_{th2} is how many times we can not get this code by using the maximum-selection method and the fixed threshold .The correlation is performed with 256 chips.

In Fig 3.13, P_{th3} means the probability of missing detection in stage3. This is calculated from a separate simulation routine where we transmit CPICH code. P_{th3} is how many times we can not get this code by using the maximum-selection method and the fixed threshold .The correlation is performed with 2560 chips.

In Fig 3.13, P_f means the probability of false alarm detection in stage1. This is calculated from a separate simulation routine where we only transmit AWGN, and we get the highest peak which is not the desired signal.

In Fig 3.13, P_{e1} means the probability of false alarm detection in stage2. This is calculated from a separate simulation routine where we transmit S-SCH code which is not the desired signal, P_{e1} is how many times we can get this code by using the maximum-selection method and the fixed threshold. The correlation is performed with 256 chips.

In Fig 3.13, P_{e2} means the probability of faise alarm detection in stage3. This is calculated from a separate simulation routine where we transmit CPICH code which is not the desired signal, P_{e2} is how many times we can get this code by using the maximum-selection method and the fixed threshold. The correlation is performed with 2560 chips.

We attempt to go to the first stage , only if we get the first code. That is if $y<1-P_{th1}$, where y is a uniformly distributed random variable between (0,1), we will go to the second stage. In the second stage we use maximum-selection method and fixed threshold. Only if we get the second code ,means $y<1-P_{th2}$, will we go to the third stage. In the third stage, and we only use maximum-selection method and fixed threshold . If acquisition fails it means $y>1-P_{th3}$, we go to stage1 again and try three times. If acquisition fails three times, we go to start. We calculate acquisition time every stage. We assume $T_1 = 10ms$[36] , $T_2 = 20ms$[36], $T_3 = 30ms$[36].

The difference between Policy 4 and Policy 3 is that we go back to branch A if y is larger than 1 - P_{th3} . In policy 3 we go back to branch E if y is larger than 1 - P_{th3} . In Policy 2 and Policy 1, we go back to the start if the condition is not satisfied.

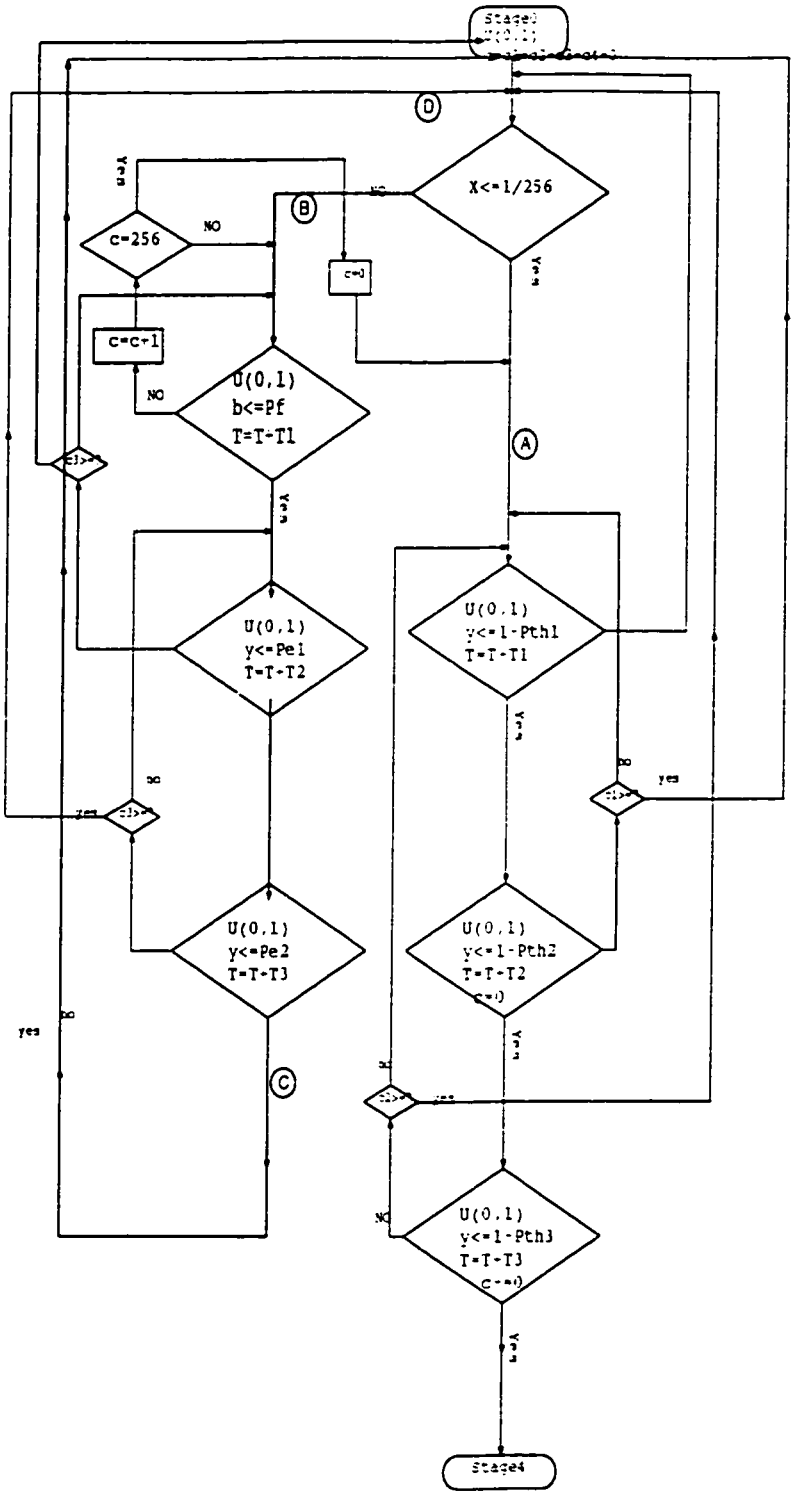

Figure 3.13: Flow Chart of Policy 4

Fifth Policy In Fig 3.14, uniformly distributed random variable y is called. If the output of this U(0,1) lies in the range [0 1/125], this means the search code phase is the correct one and so the simulation program proceeds to branch A. If the output of U(0,1) lies outside the range [1, 1/125], the simulation program continues to branch B which then adds T_1, T_2 and T_3 to the failed acquisition trials and the flow chart gets finally to branch C, and where U(1,0) is called again. Similarly continuing from branch A, U(0,1) is called and T_1, T_2 and T_3 are added to the acquisition time counter for first time. After first time, only T_3 is added to the acquisition time counter.

In Fig 3.14, P_{m1} means the probability of missing detection in stage1. This is calculated from a separate simulation routine where we transmit P-SCH code , P_{m1} is how many times we can not get this code by using match filter.

In Fig 3.14, P_{m2} means the probability of missing detection in stage2. This is calculated from a separate simulation routine where we transmit S-SCH code. P_{m2} is how many times we can not get this code by using maximum detection method (no thresholds set over correlators outputs). The correlation is performed with 256 chips.

In Fig 3.14, P_{m3} means the probability of missing detection in stage3. This is calculated from a separate simulation routine where we transmit CPICH code. P_{m3} is how many times we can not get this code by using the maximum detection method (no thresholds set over correlators outputs).The correlation is performed with 2560 chips.

In Fig 3.14, P_f means the probability of false alarm detection in stage1. This is calculated from a separate simulation routine where we only transmit AWGN, and we get the highest peak which is not the desired signal.

In Fig 3.14, P_{e1} means the probability of false alarm detection in stage2. This is calculated from a separate simulation routine where we transmit S-SCH code which is not the desired signal. P_{e1} is how many times we can get this code by

using maximum-selection method (no thresholds set over correlators outputs). The correlation is performed with 256 chips.

In Fig 3.14 P_{e2} means the probability of false alarm detection in stage3. This is calculated from a separate simulation routine where we transmit CPICH code which is not the desired signal, P_{e2} is how many times we can get this code by using maximum-selection method (no thresholds set over correlators outputs). The correlation is performed with 2560 chips.

We use a pipelined way to search. We attempt to go to the first stage, only if we get the first code. If $y<1-P_{m1}$, where y is a uniformly distributed random variable between (0,1), we will go to the second stage. Otherwise we go to start . In the second stage, we use maximum-selection method and no fixed threshold. Only if we get the second code, that is $y<1-P_{m2}$, will we go to the third stage. otherwise we go to start . In the third stage, we only use maximum-selection method and no fixed threshold . If acquisition fails it means $y>1-P_{m3}$, and we go to start. We calculate acquisition time first process and other process we only calculate the third stage acquisition time . We assume the first stage acquisition time $T_1 = 10ms$[36] , the second stage acquisition time $T_2 = 20ms$[36], and the third stage acquisition $T_3 = 30ms$[36].

The difference between Policy 5 and the other four policies is the use of a pipelined search. Policy 4, Policy 3, Policy 2 and Policy 1 all use serial search.

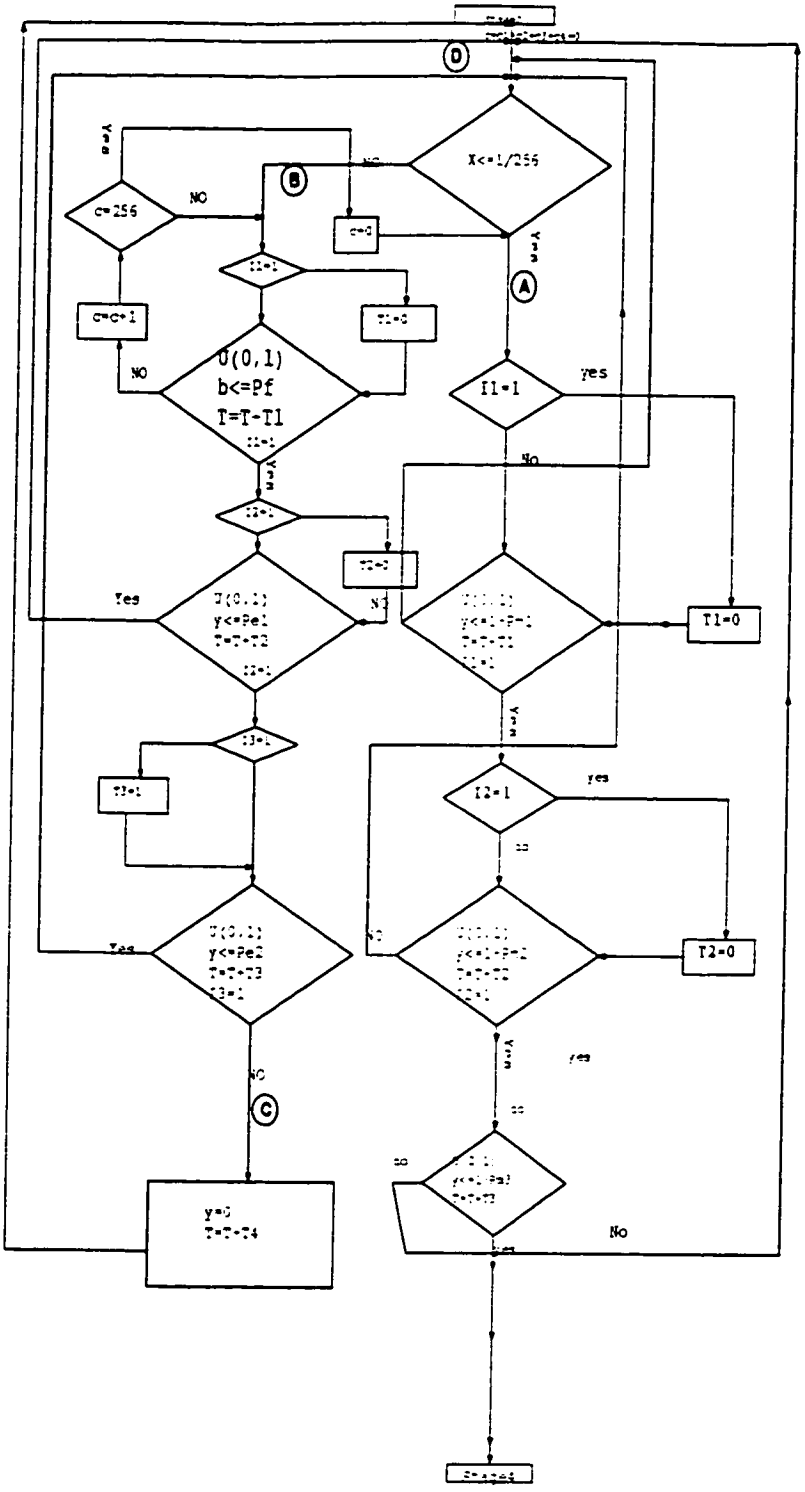

Figure 3.14: Flow Chart of Policy 5

Sixth Policy In Fig 3.15, uniformly distributed random variable y is called. If the output of this U(0,1) lies in the range [0 1/125], this means the search code phase is correct one and so the simulation program proceeds to branch A. If the output of U(0,1) lies outside the range [1, 1/125],the simulation program continues to branch B which then adds T_1, T_2 and T_3 to the failed acquisition trials and the flow chart gets finally to branch C, where U(1,0) is called again. Similarly continuing from branch A, U(0,1) is called and T_1, T_2 and T_3 are added to the acquisition time counter for the first time. After the first time, only T_3 is added to the acquisition time counter.

In Fig 3.15, P_{th1} means the probability of missing detection in stage1. This is calculated from a separate simulation routine where we transmit P-SCH code , P_{th1} is how many times we can not get this code by using match filter.

In Fig 3.15, P_{th2} means the probability of missing detection in stage2. This is calculated from a separate simulation routine where we transmit S-SCH code. P_{th2} is how many times we can not get this code by using the maximum detection method and the fixed threshold.The correlation is performed with 256 chips.

In Fig 3.15, P_{th3} means the probability of missing detection in stage3. This is calculated from a separate simulation routine where we transmit CPICH code. P_{th3} is how many times we can not get this code by using the maximum detection method and the fixed threshold.The correlation is performed with 2560 chips.

In Fig 3.15, P_f means the probability of false alarm detection in stage1. This is calculated from a separate simulation routine where we only transmit AWGN, and we get the highest peak which is not the desired signal.

In Fig 3.15, P_{e1} means the probability of false alarm detection in stage2. This is calculated from a separate simulation routine where we transmit S-SCH code which is not the desired signal, P_{e1} is how many times we can get this code by using the maximum-selection method and the fixed threshold. The correlation is performed with 256 chips.

In Fig 3.15, P_{e2} is the probability of false alarm detection in stage3. This is calculated from a separate simulation routine where we transmit CPICH code which is not the desired signal, P_{e2} is how many times we can get this code by using the maximum-selection method and the fixed threshold. The correlation is performed with 2560 chips.

We use a pipelined way to search.We attempt to go to the first stage, only if we get the first code. If y<1-P_{th1}, where y is a uniformly distributed random variable between (0,1), we will go to the second stage. Otherwise we go to start . In the second stage,we use maximum-selection method and fixed threshold. Only if we get the second code which means y<1-P_{th2}, we will go to the third stage.otherwise we go to start . In the third stage, we only use maximum-selection method and fixed threshold . If acquisition fails it means y>1-P_{th3}, we go to start. We calculate acquisition time first process and other process we only calculate the third stage acquisition time . We assume the first stage acquisition time $T_1 = 10ms$[36] , the second stage acquisition time $T_2 = 20ms$[36], and the third stage acquisition $T_3 = 30ms$[36].

The difference between Policy 6 and Policy 5 is that we use a fixed threshold in stage2 and stage3. Policy 6 uses the pipelined search.

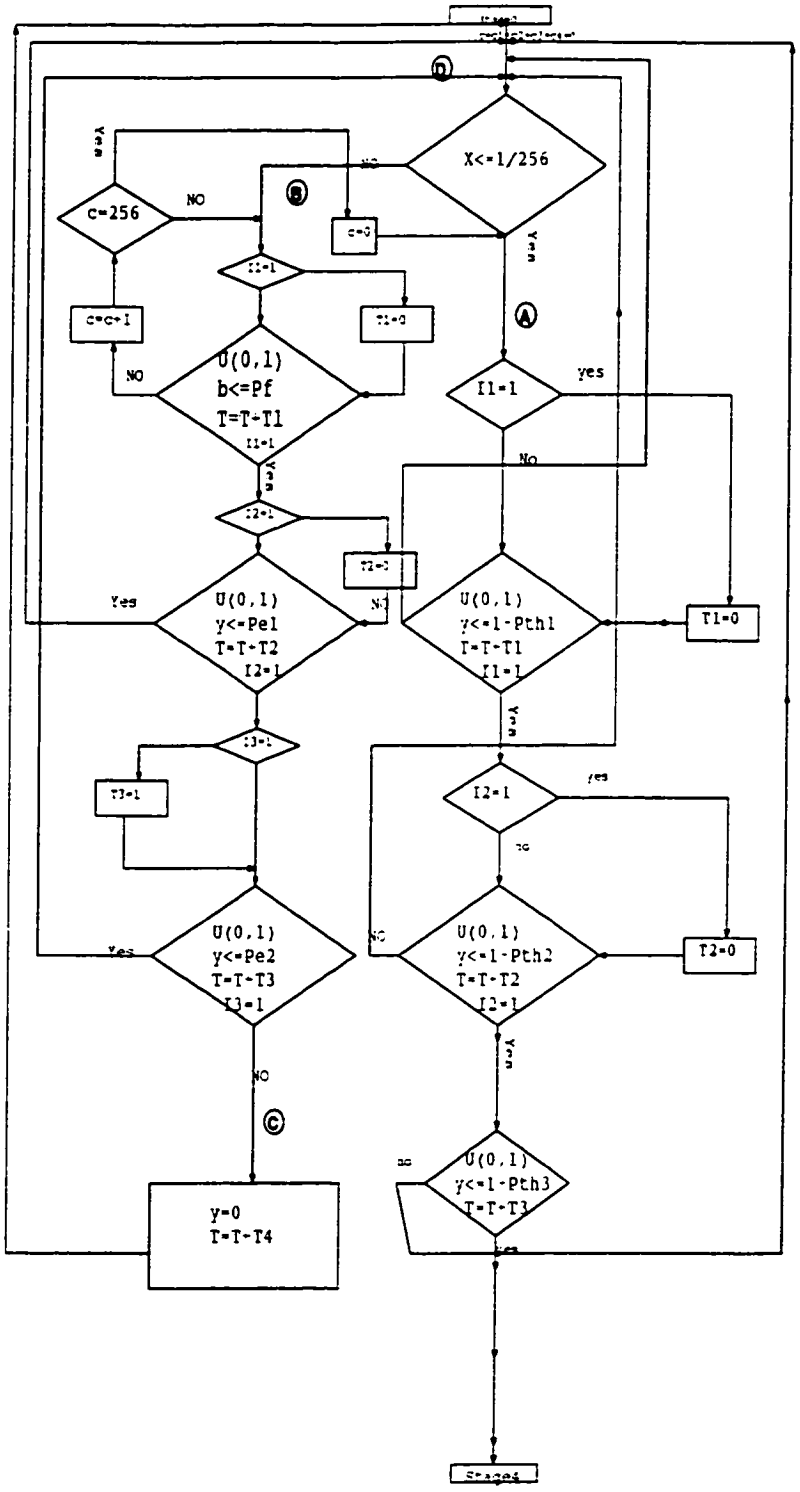

Figure 3.15: Flow Chart of Policy 6

Case I

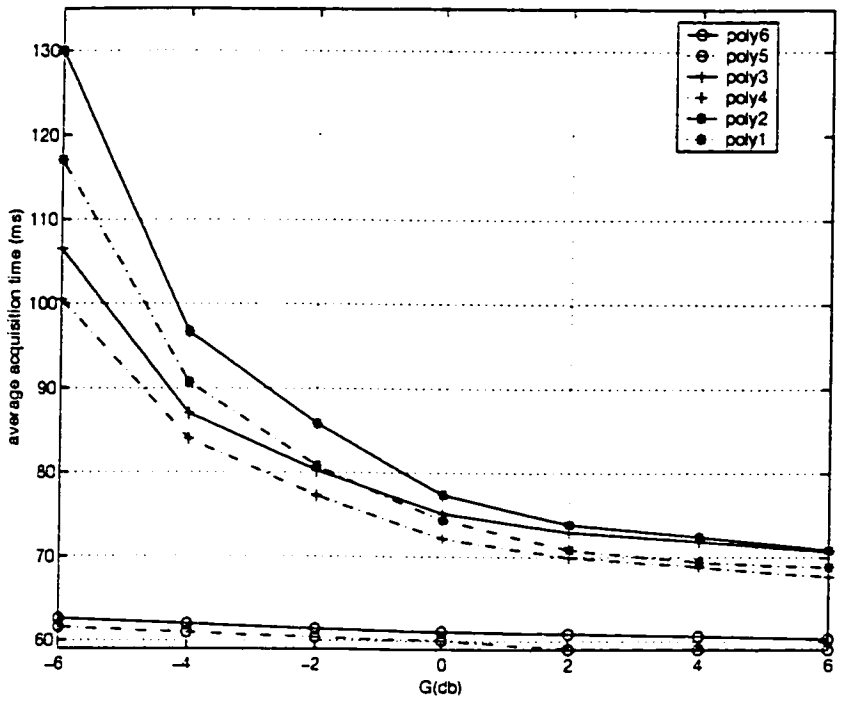

Figure 3.16: Average acquisition time in flat fading channel (8km/h)

Fig 3.16 shows that average acquisition times for Policy1, Policy2, Policy3, Policy4, Policy5 and Policy6 in flat fading channel (with MS at 8km/h), decreases with G [37](G is defined below). The superiority of our new pipeline Policies 5 and 6 are clear. The average acquisition time of any policy is calculated from flow charts of Fig 3.13, Fig 3.14 and Fig 3.15, where T_1, T_2 and T_3 are added to T depending on the outcome of each stage. G means the ratio between the power of the desired base stations signal and the postchannel interference, i.e., $G = (P_1 + P_2 + P_3 + P_I)/P_x$, where P_1 is power of P-SCH, P_2 is power of S-SCH, P_3 is power of CPICH, P_I is power of intra-cell interference and P_x is power of inter-cell interference.

Case II

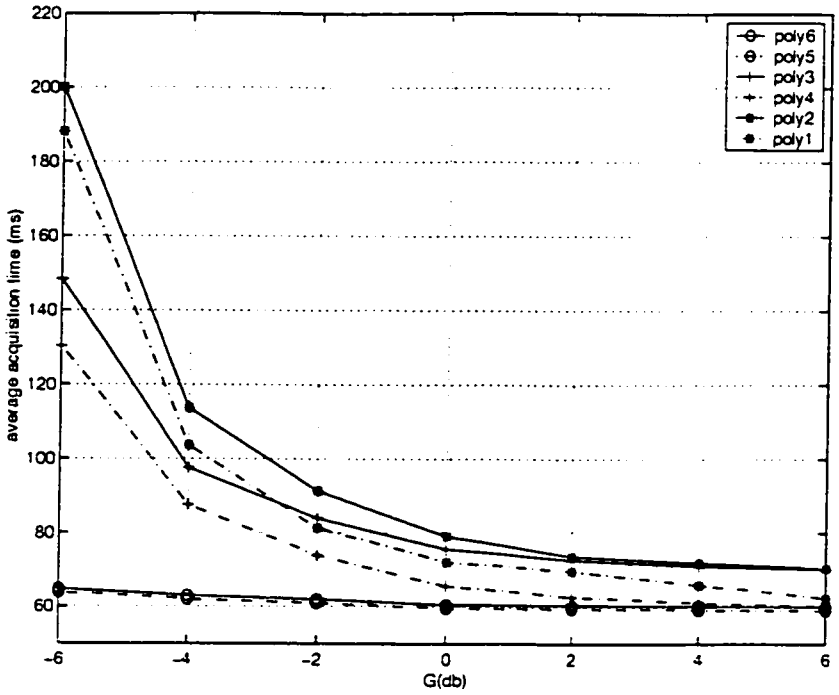

Figure 3.17: Average acquisition time in flat fading channel (80km/h)

Fig 3.17 shows the superiority of our new pipeline Policy5 and Policy 6. The average acquisition time of every policy is a little larger than those in Fig 3.16. G has the same meaning as before.

We have two cases in frequency selective fading channel: CASE I (Vehicular, 8km/h), CASE II (Vehicular, 80 km/h) .

Case I

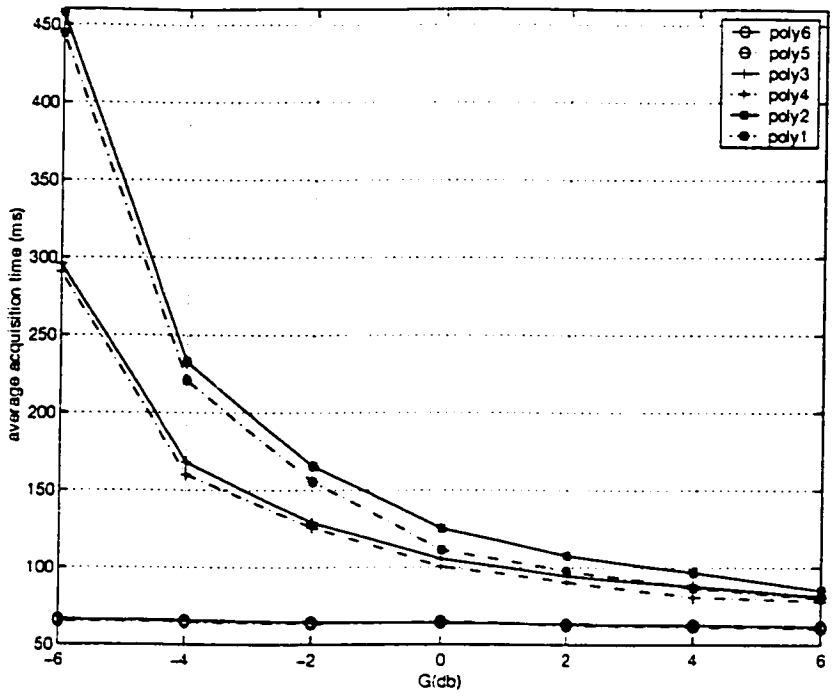

Figure 3.18: Average acquisition time in frequency selective fading channel (8km/h)

Fig 3.18 shows the results for Policy1, Policy2, Policy3, Policy4, Policy5 and Policy6 in frequency selective fading channel, with MS moving at 8km/h. The superiority of our new pipeline Policy5 and Policy6 is clear. The average acquisition time of any policy is calculated from Fig 3.10, Fig 3.11, Fig 3.12, Fig 3.13, Fig 3.14 ,Fig 3.15, where T_1, T_2 and T_3 are added to T depending on the outcome of each stage.

The average acquisition time of every policy is higher than those in Fig 3.16 and Fig3.17. G is the same meaning as before, due to frequency selectivity.

Case II

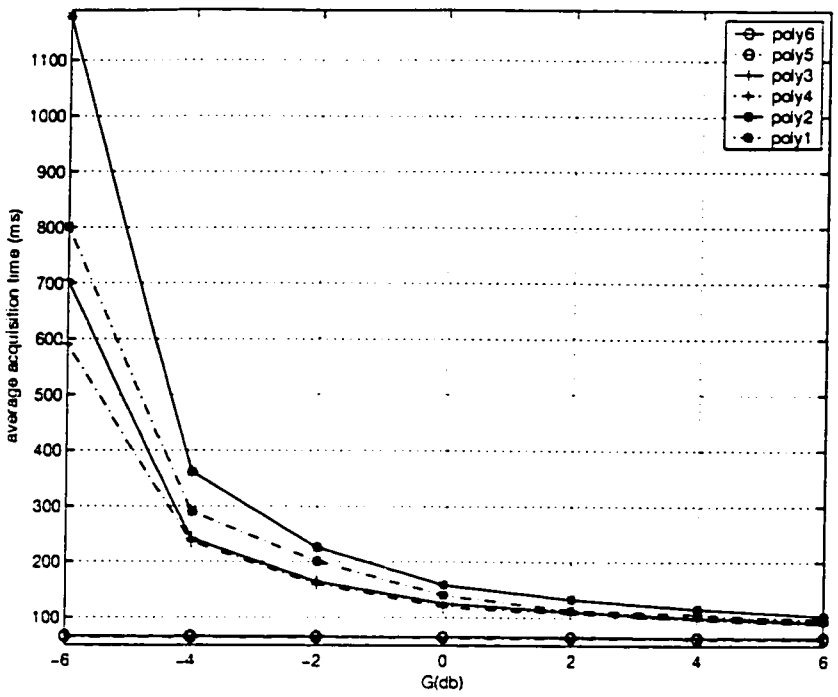

Figure 3.19: Average acquisition time in frequency selective fading channel (80km h)

Fig 3.19 shows the results for Policy1, Policy2, Policy3, Policy4, Policy5 and Policy6 in flat fading channel, with MS moving at 8km/h decreases with G. The superiority of our new pipeline Policy5 and Policy6 is clear. The average acquisition time of any policy is calculated from Fig 3.16, Fig3.17, Fig3.18, where T_1, T_2 and T_3 are added to T depending on the outcome of each stage.

The average acquisition time of every policy is higher than those in Fig 3.16, Fig 3.17 and Fig 3.18. G has the same meaning as before.

3.3 Threshold Selection and Acquisition time

In this part of simulation , we try to find the effect of changing the threshold on the acquisition performance. Four of the policies have a threshold associated with them namely Policy2, Policy3, Policy4 and Policy6. We are trying to find a way to do this. We got all the parameters P_{fa} (probability of false alarm) , P_D(probability

of detection) , P_e(probability of missing) , P_{th} (probability of detection in fixed threshold) from our model.

Fig 3.20 shows the existence of an optimum threshold which gets larger as G increases in the range(-6,-4,0,2) in the case of Policy2.

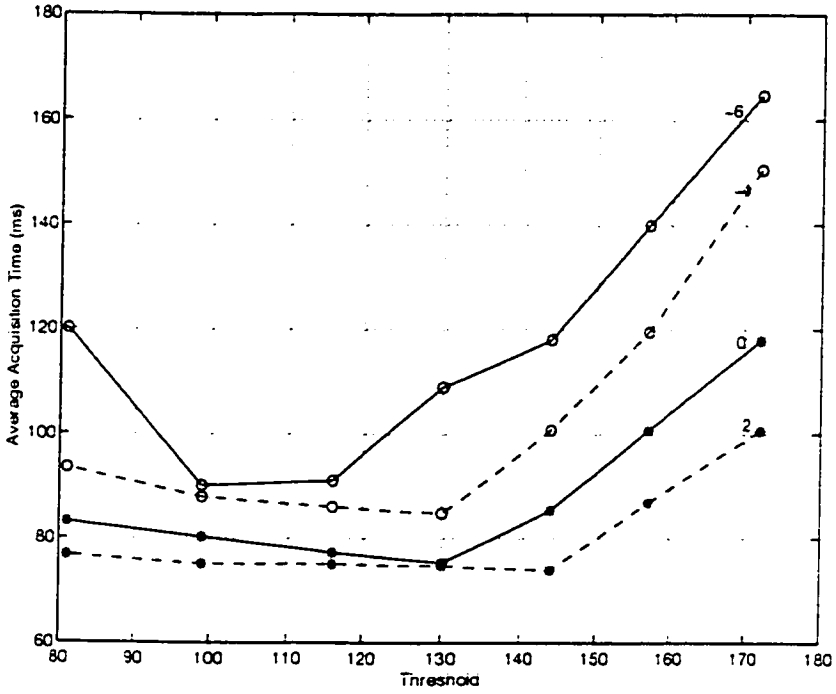

Figure 3.20: Acquisition time of Policy2 in Flat Fading Channel (8km/h)

Fig 3.21 shows the existence of an optimum threshold which gets larger as G increases in the range(-6,-4,0,2) in the case of Policy3.

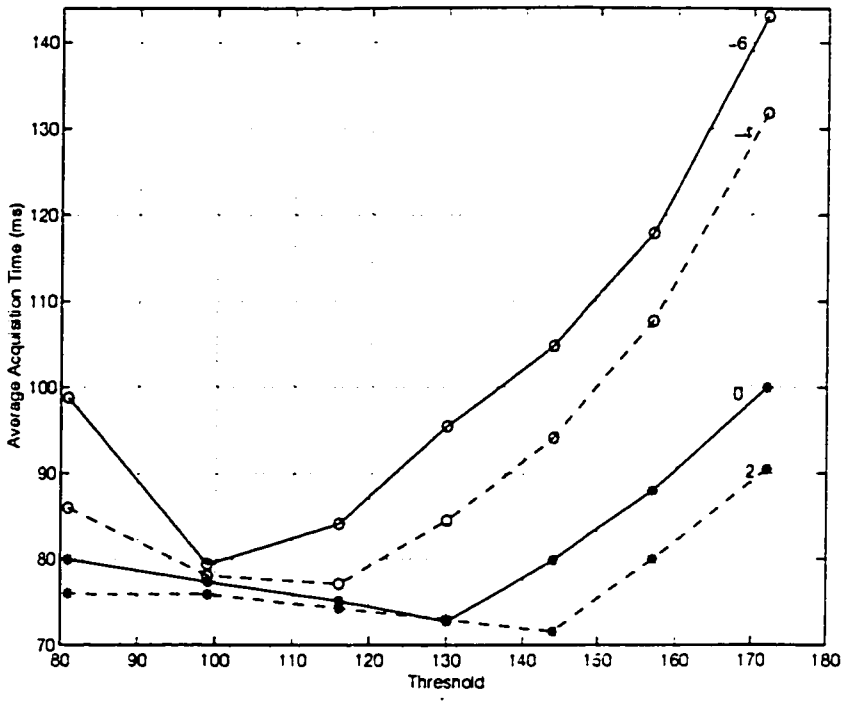

Figure 3.21: Acquisition time of Policy3 in Flat Fading Channel (8km/h)

Fig 3.22 shows the existence of an optimum threshold which gets larger as G increases in the range(-6,-4,0,2) in the case of Policy4. Fig 3.23 shows the existence of an optimum threshold which gets larger as G increases in the range(-6,-4,0,2) in the case of Policy6. Moreover, comparing Fig 3.23 to earlier Fig 3.20 we see that Policy2 shows the better result as the threshold are optimized. Fig 3.24 shows the existence of an optimum threshold which gets larger as G increases in the range(-6,-4,0,2) in the case of Policy2. Fig 3.25 shows the existence of an optimum threshold which gets larger as G increases in the range(-6,-4,0,2) in the case of Policy3. Fig 3.26 shows the existence of an optimum threshold which gets larger as G increases in the range(-6,-4,0,2) in the case of Policy4. Fig 3.27 shows the existence of an optimum threshold which gets larger as G increases in the range(-6,-4,0,2) in the case of Policy6. Moreover, comparing Fig 3.27 to Fig 3.24, we see that Policy6 shows better results as the thresholds are optimized. Fig 3.28 shows the existence

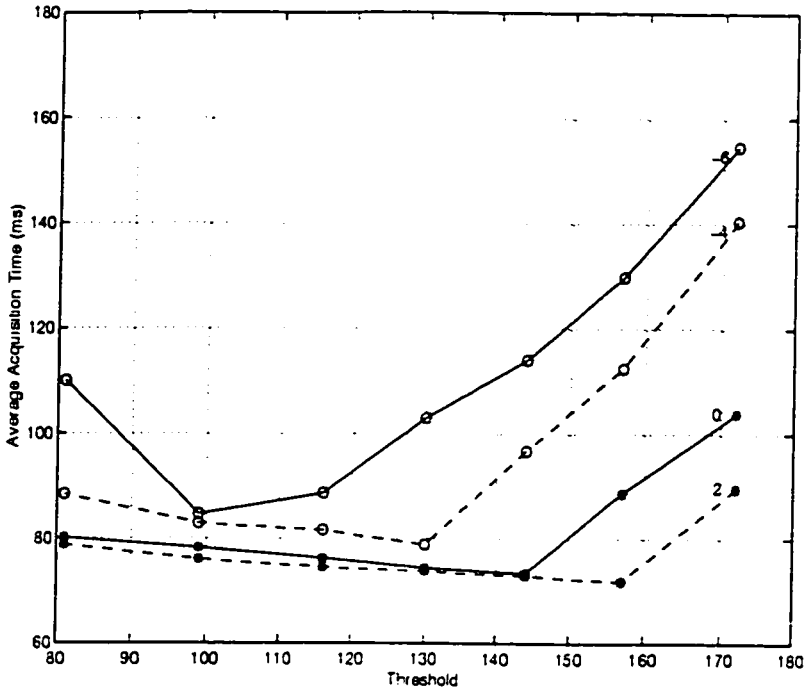

Figure 3.22: Acquisition time of Policy4 in Flat Fading Channel (8km/h)

of an optimum threshold which gets larger as G increases in the range(-6,-4,0,2) in the case of Policy2. Fig 3.29 shows the existence of an optimum threshold which gets larger as G increases in the range(-6,-4,0,2) in the case of Policy3. Fig 3.30 shows the existence of an optimum threshold which gets larger as G increases in the range(-6,-4,0,2) in the case of Policy4. Fig 3.31 shows the existence of an optimum threshold which gets larger as G increases in the range(-6,-4,0,2) in the case of Policy6. Moreover, comparing Fig3.30 to earlier Fig 3.30 we see that Policy6 shows the better result as the threshold are optimized. Fig 3.32 shows the existence of an optimum threshold which gets larger as G increases in the range(-6,-4,0,2) in the case of Policy2. Fig 3.33 shows the existence of an optimum threshold which gets larger as G increases in the range(-6,-4,0,2) in the case of Policy3. Fig 3.34 shows the existence of an optimum threshold which gets larger as G increases in the range(-6,-4,0,2) in the case of Policy4.

Fig 3.35 shows the existence of an optimum threshold which gets larger as G

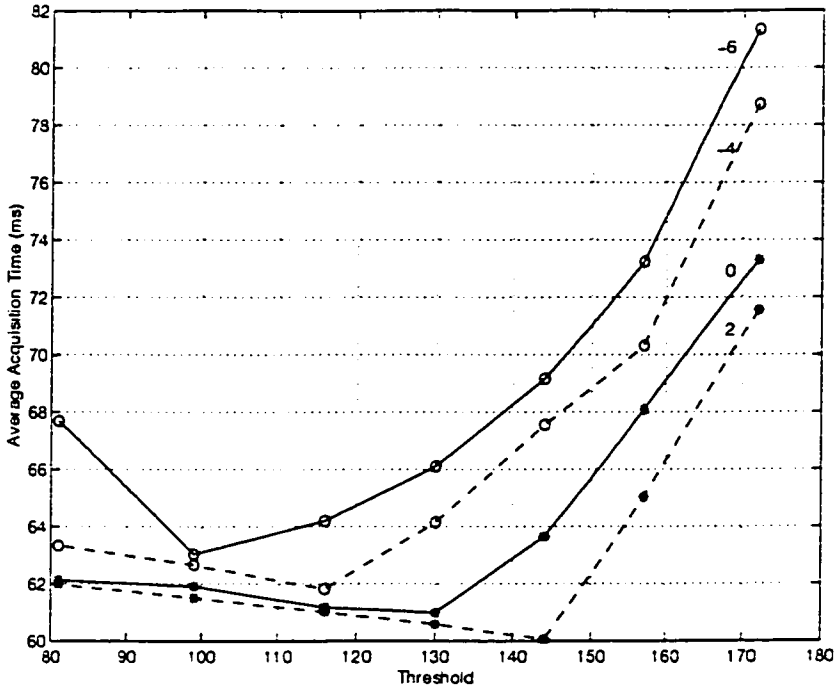

Figure 3.23: Acquisition time of Policy6 in Flat Fading Channel (8km h)

increases in the range(-6,-4,0,2) in the case of Policy6. Moreover, comparing Fig 3.35 to earlier Fig 3.32 we see that Policy6 shows better results as the threshold are optimized. We found that these figures show that acquisition time depends on the pattern distributions of P_{fa} and P_d . Numerical results give insight onto the impact of different system parameters on the system performance, especially the importance of proper decision threshold setting.

3.4 SNR and Variance of the Acquisition time

We are interested in different acquisition policies and multipath fading in our model. In this work, we have also computed the variance of the code acquisition time for all six policies and all fading channels. Fig 3.36 shows a sample of the result obtained. For all variances with different G, our Policy6 yields minimum variance in all policies.

Fig 3.37 shows a sample of the result obtained. For all variances with different

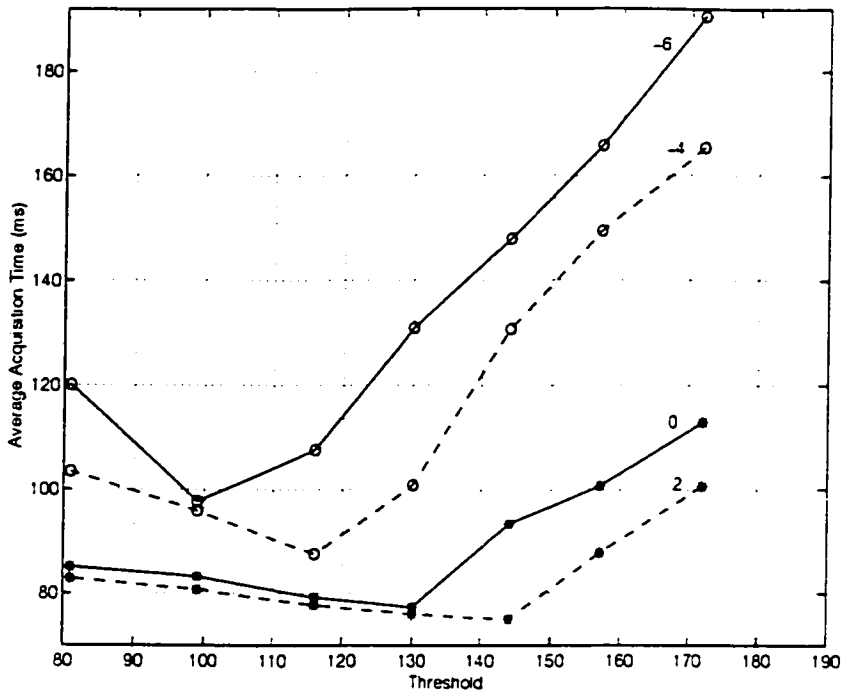

Figure 3.24: Acquisition time of Policy2 in Flat Fading Channel (80km/h)

G, our Policy6 yields minimum variance in all policies. Fig 3.38 shows a sample of the result obtained. For all variances with different G, our Policy6 yields minimum variance in all policies.

Fig 3.39 shows a sample of the result obtained. For all variances with different G, our Policy6 yields minimum variance in all policies.

From the last section, we obtained variance of acquisition time in different channels and different G. We found that the acquisition time changes faster in frequency-selective fading channel. Policy6 yielded best result with less sensitivity to G.

We found that Policy2, Policy3 and Policy4 have similar trends in different SNR. Our policy (Policy 6) is more stable in different channels. We found the variance of acquisition time changes more in Policy2, Policy3 and Policy4.

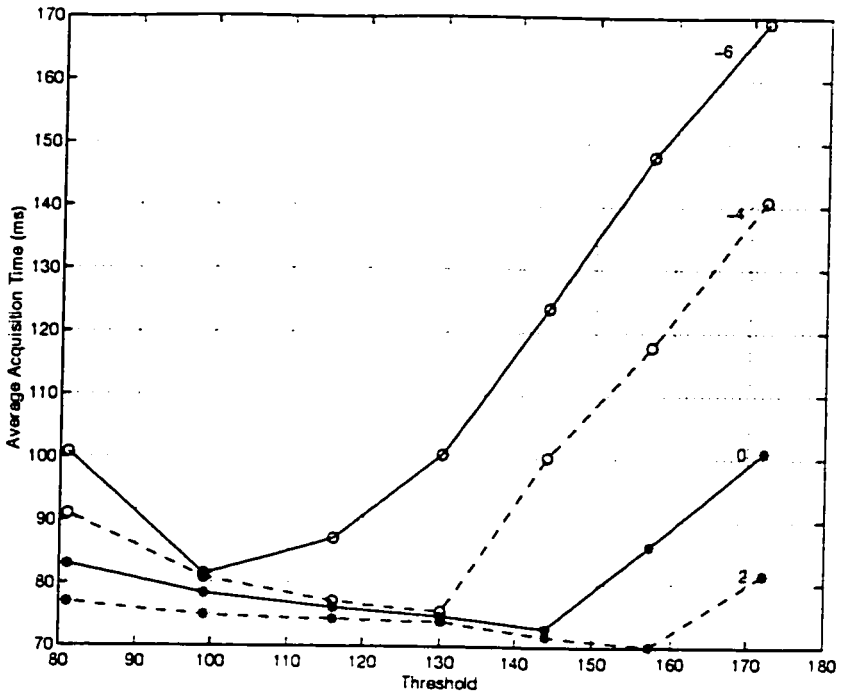

Figure 3.25: Acquisition time of Policy3 in Flat Fading Channel (80km/h)

3.5 Comparison

In this work we have also compared the threshold effects on all 6 policies.Fig 3.40 shows a sample of such result: our Policy6 yields the result in frequency selective fading channel(80km/h). In general Policy3 is better than Policy4, but see Fig3.40. We found that the channel condition is an important factor in determining the average acquisition time.

Fig 3.41 shows a sample of such result: our policy6 yields the best results in flat fading(8km/h). Fig 3.42 shows a sample of such result: our policy6 yields the best results in flat fading(80km/h).

By using these results, we can elaborate upon different policies for synchronization and analyze the average acquisition time. For higher SNR, the range of optimal threshold is wider. These results can be used to create a look up table for optimal threshold settings. One should be aware that in the case of imperfect code synchronization P_D should be modified by SNR through the threshold adjustment.

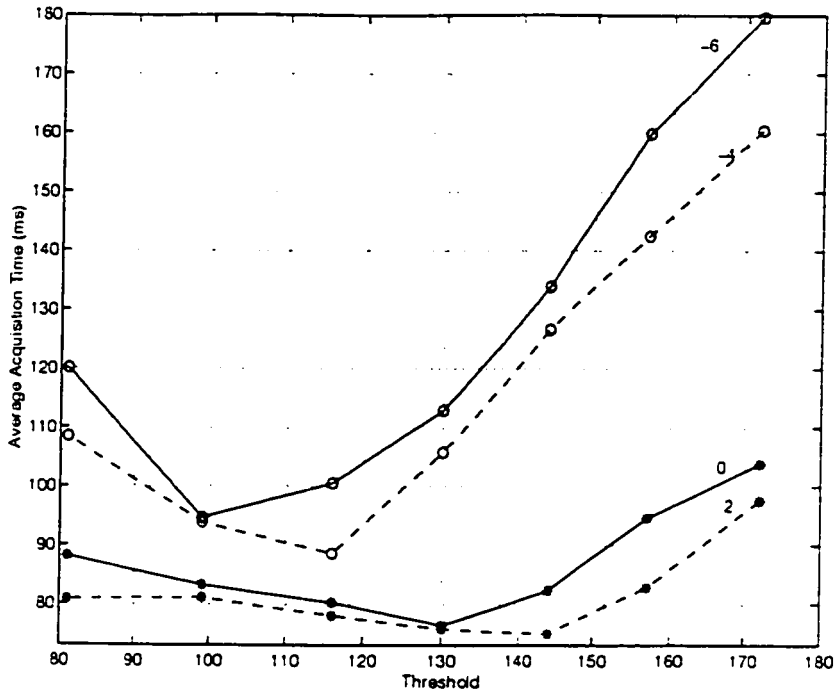

Figure 3.26: Acquisition time of Policy4 in Flat Fading Channel (80km h)

A new method of cell search code acquisition process has been introduced. Our Policy6 is better than other policies. It was seen that the acquisition performance depends on the search strategy employed as well as threshold adjustment.

In general, Policy3 is better than Policy4. In general Policy3 is better than Policy4, but see Fig4.10. We found that the channel condition is an important factor in determining the acquisition time. Fig 3.42 shows a sample of this result: our Policy6 yields the best result in frequency-selective fading(8km/h). We found the threshold does not change a lot when mobile speed change more, so we can ignore the effect of the mobile speed to the threshold.

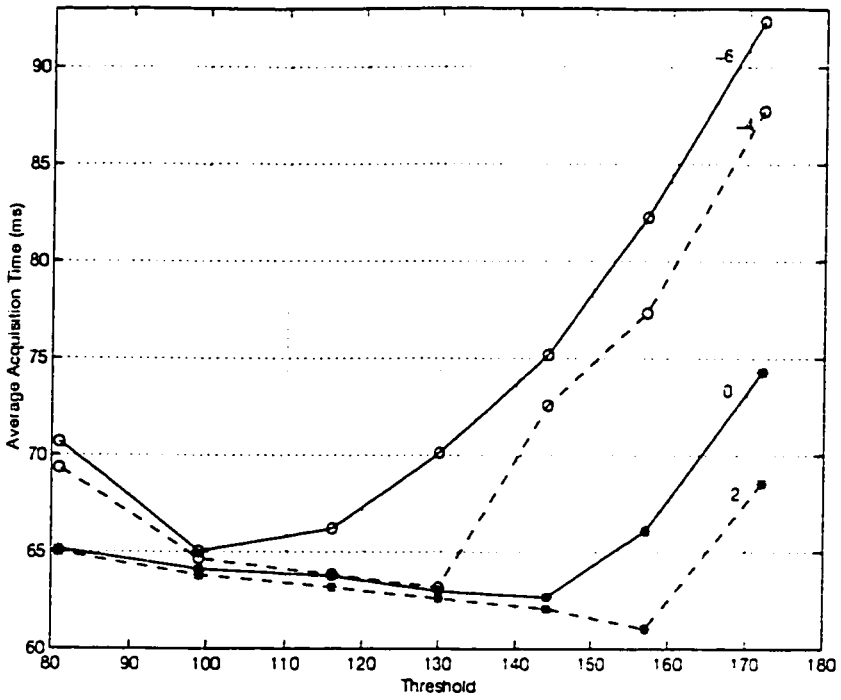

Figure 3.27: Acquisition time of Policy6 in Flat Fading Channel (80km/h)

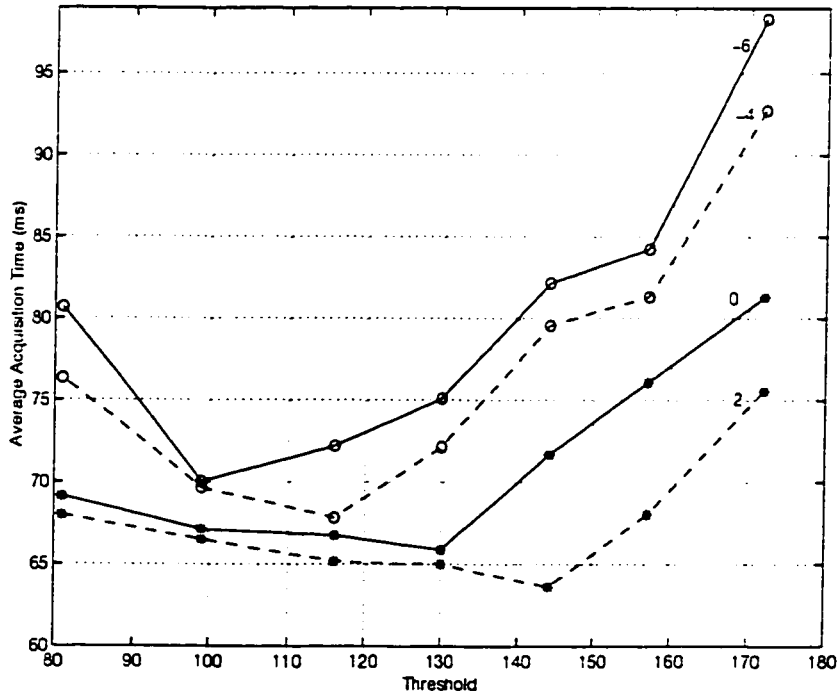

Figure 3.28: Acquisition time of Policy2 in Frequency-Selective Fading Channel (8km/h)

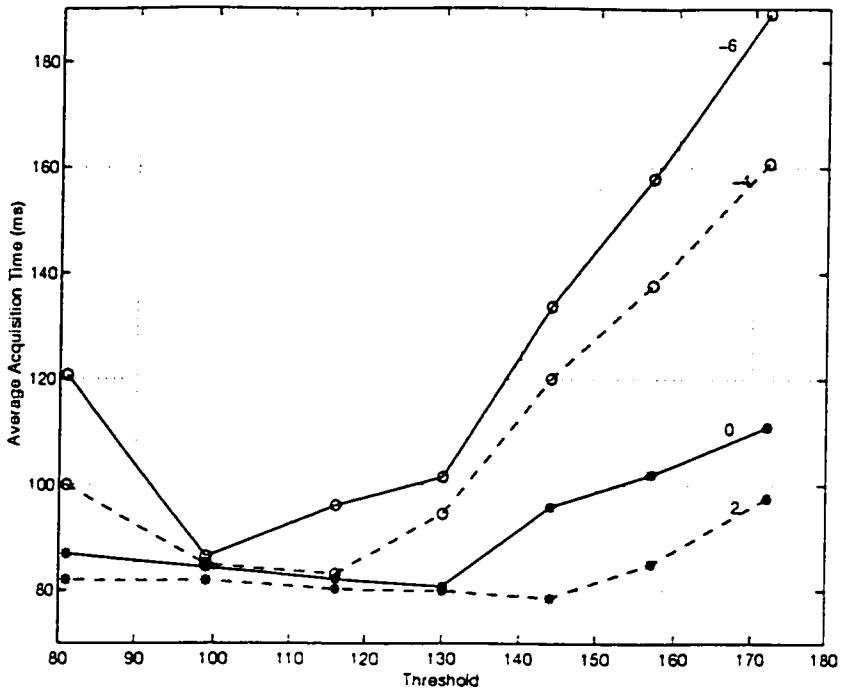

Figure 3.29: Acquisition time of Policy3 in Frequency-Selective Fading Channel (8km/h)

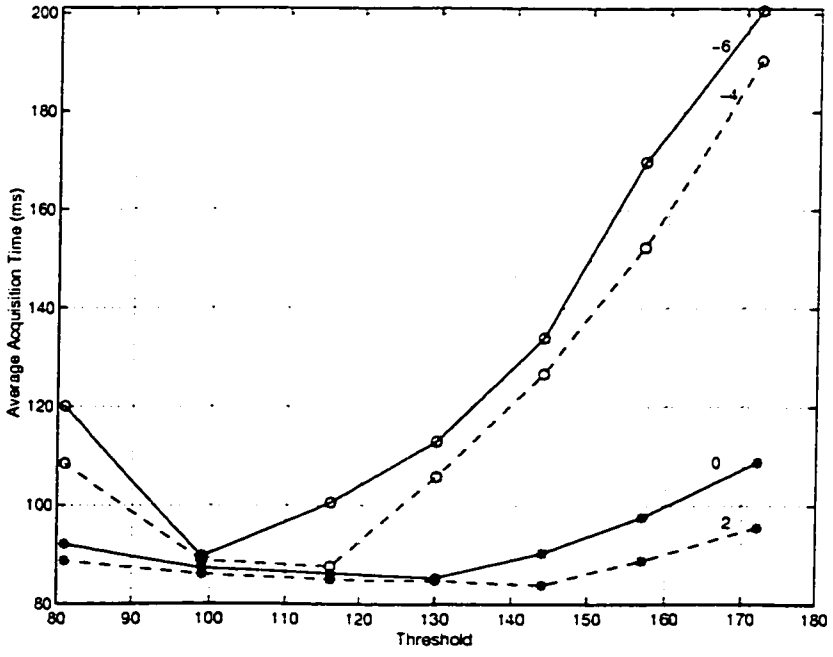

Figure 3.30: Acquisition time of Policy4 in Frequency-Selective Fading Channel (8km/h)

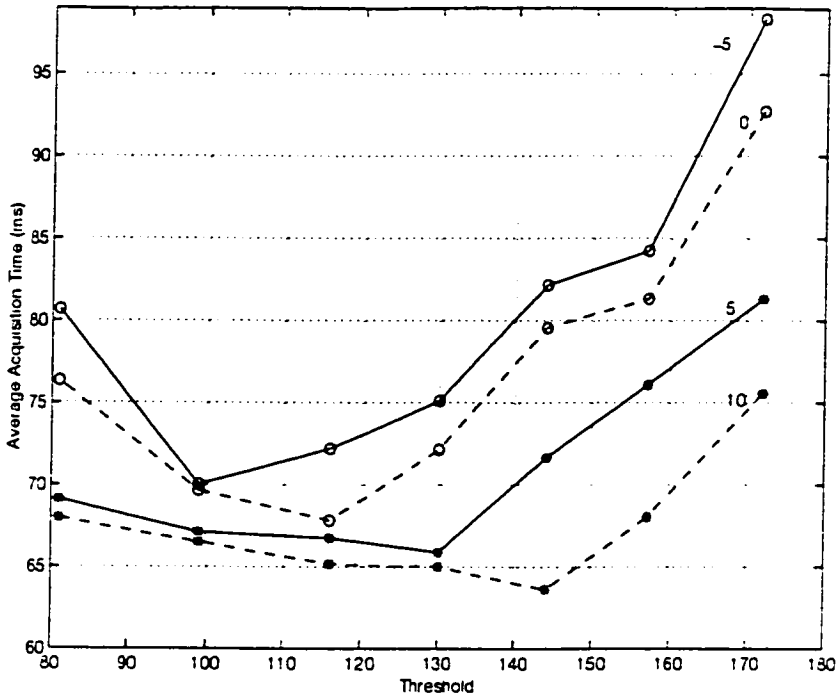

Figure 3.31: Acquisition time of Policy6 in Frequency-Selective Fading Channel (8km h)

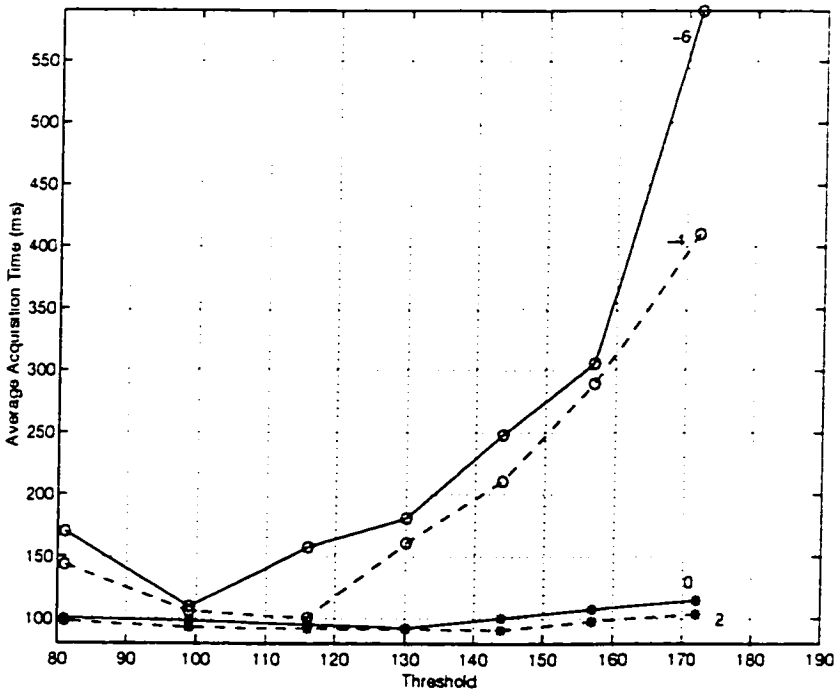

Figure 3.32: Acquisition time of Policy2 in Frequency-Selective Fading Channel (80km/h)

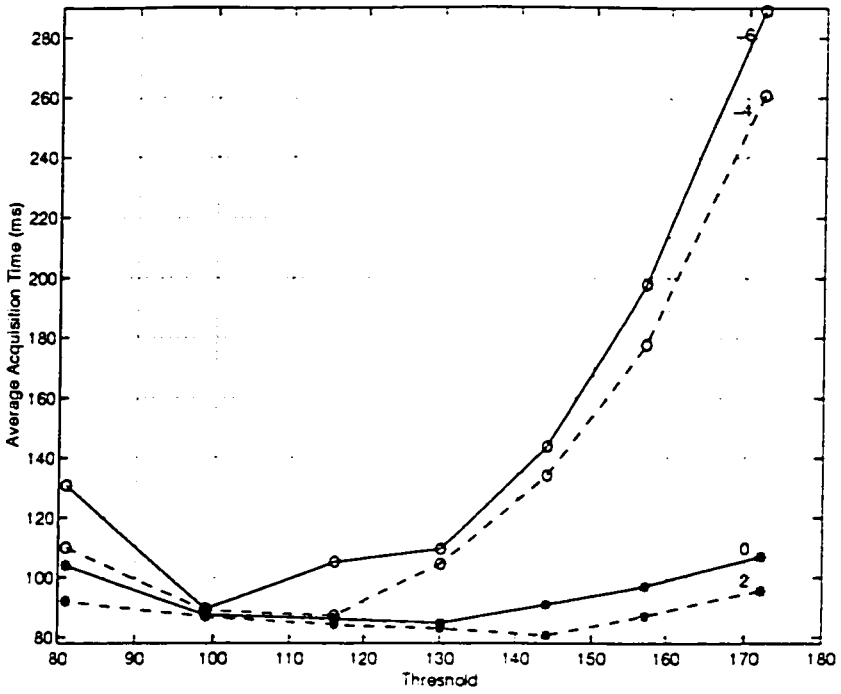

Figure 3.33: Acquisition time of Policy3 in Frequency-Selective Fading Channel (80km/h)

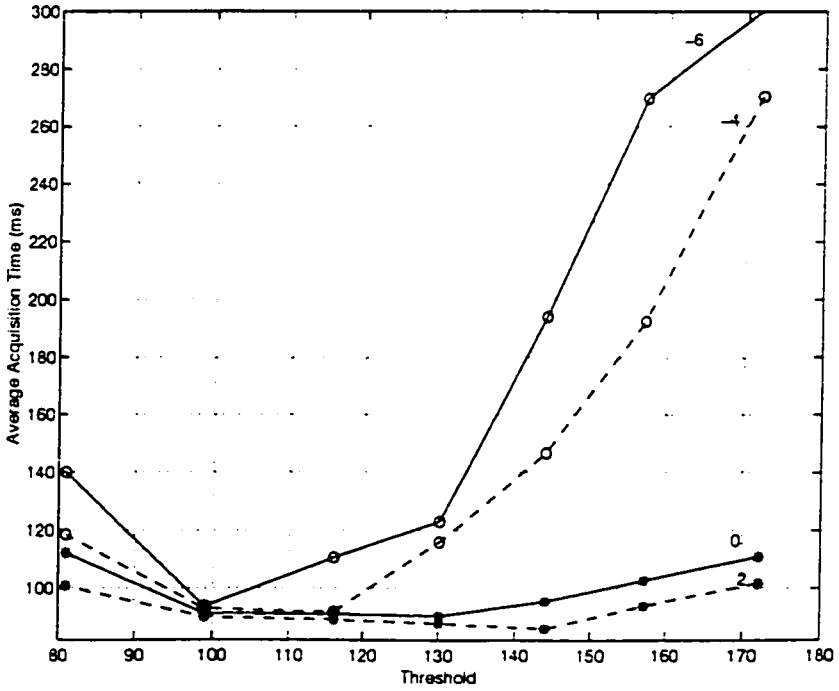

Figure 3.34: Acquisition time of Policy4 in Frequency-Selective Fading Channel (80km/h)

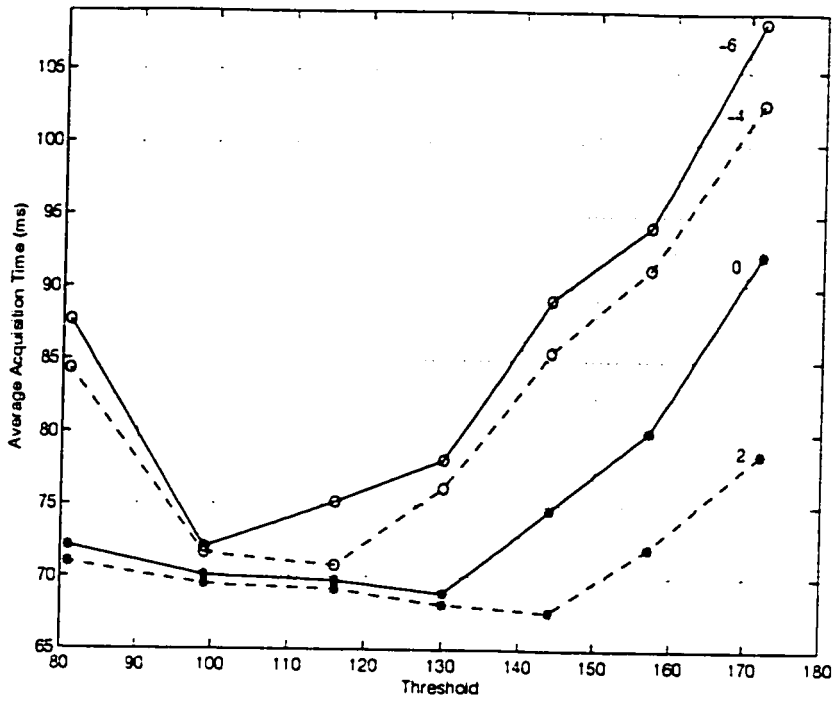

Figure 3.35: Acquisition time of Policy6 in Frequency-Selective Fading Channel (80km/h)

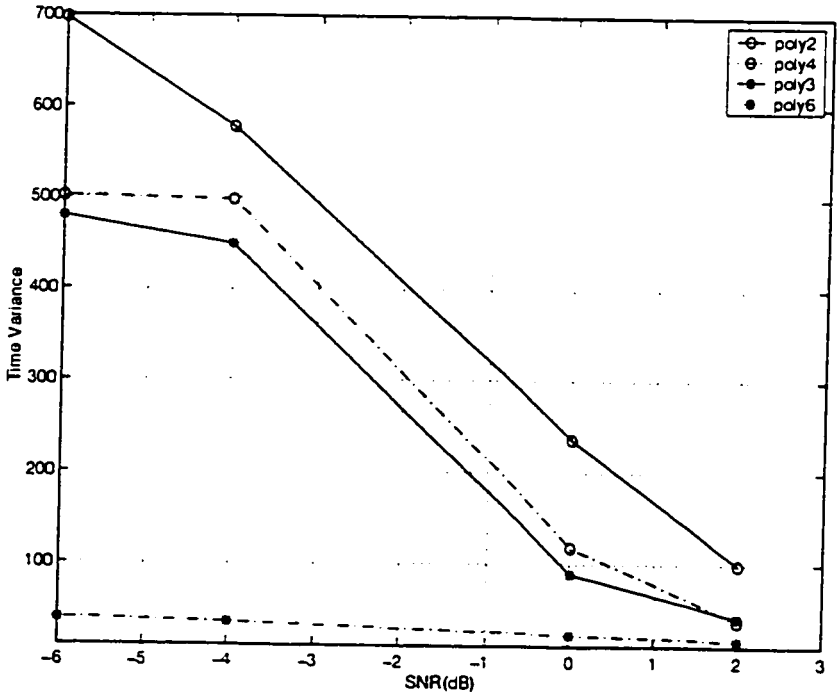

Figure 3.36: Variance of Acquisition Time in Flat Fading Channel(8km h)

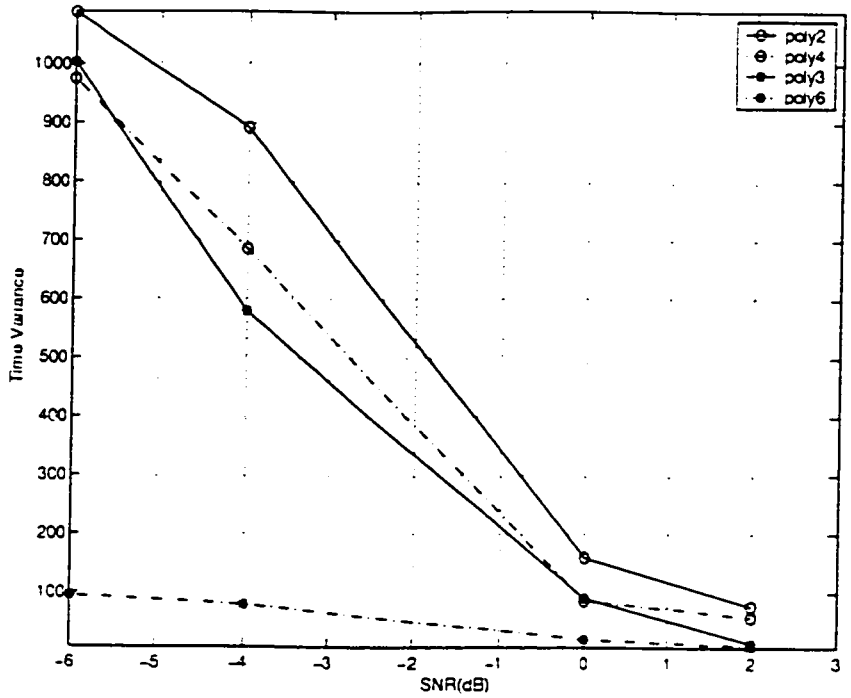

Figure 3.37: Variance of Acquisition Time in Flat Fading Channel(80km h)

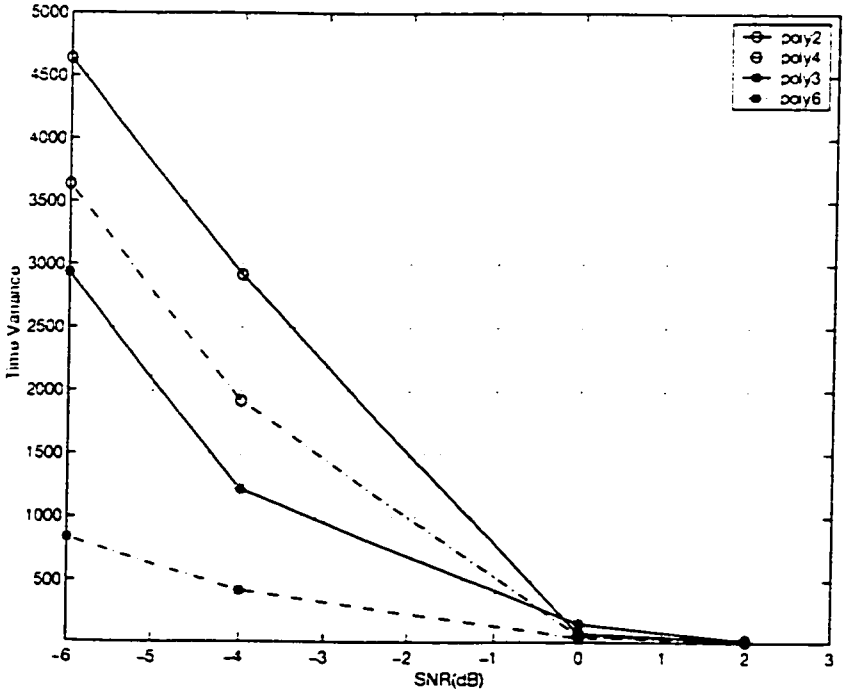

Figure 3.38: Variance of Acquisition Time in Frequency-selective Fading Channel (8km/h)

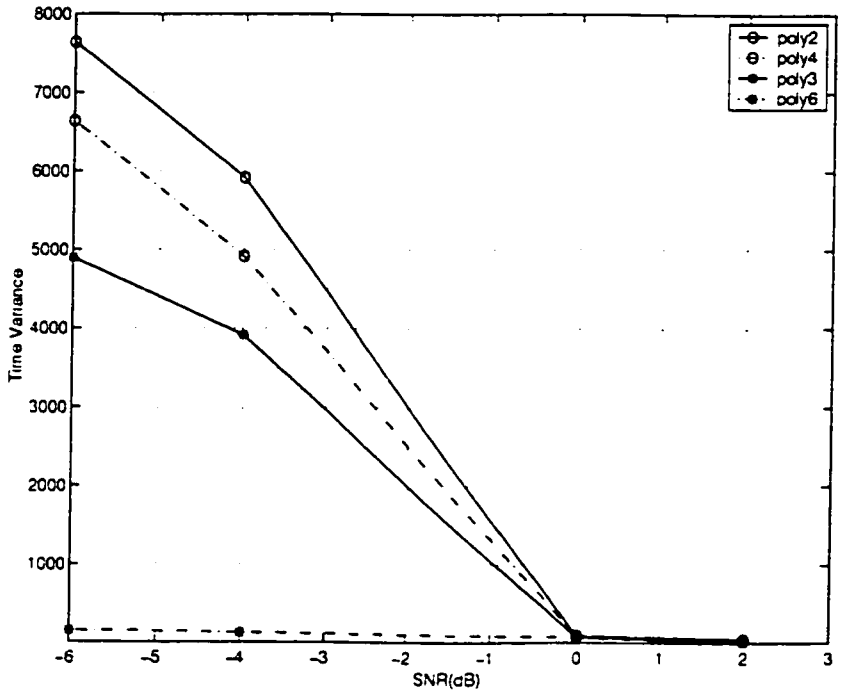

Figure 3.39: Variance of Acquisition Time in Frequency-selective Fading Channel (80km/h)

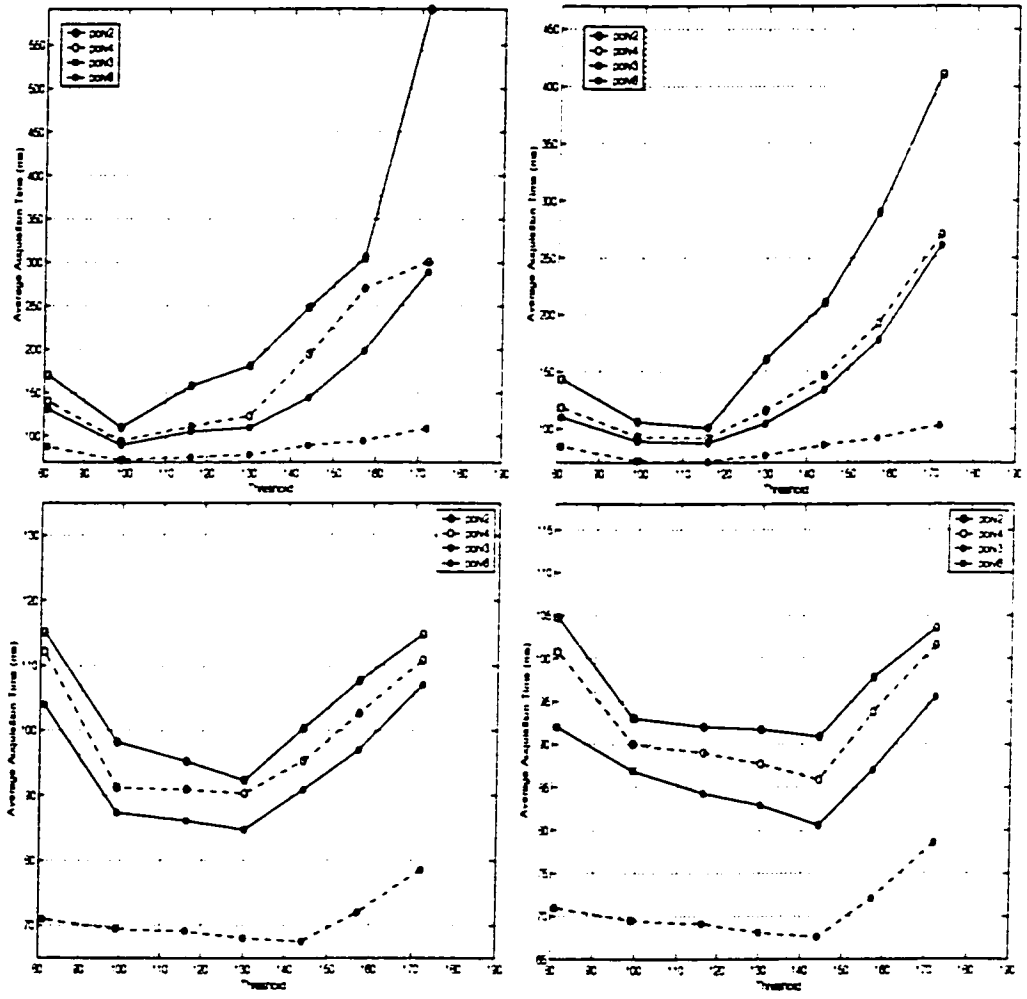

Figure 3.40: Acquisition Time of Different Policies in Frequency-Selective Fading Channel (80km/h)(SNR=-6,-4,0,2 dB)

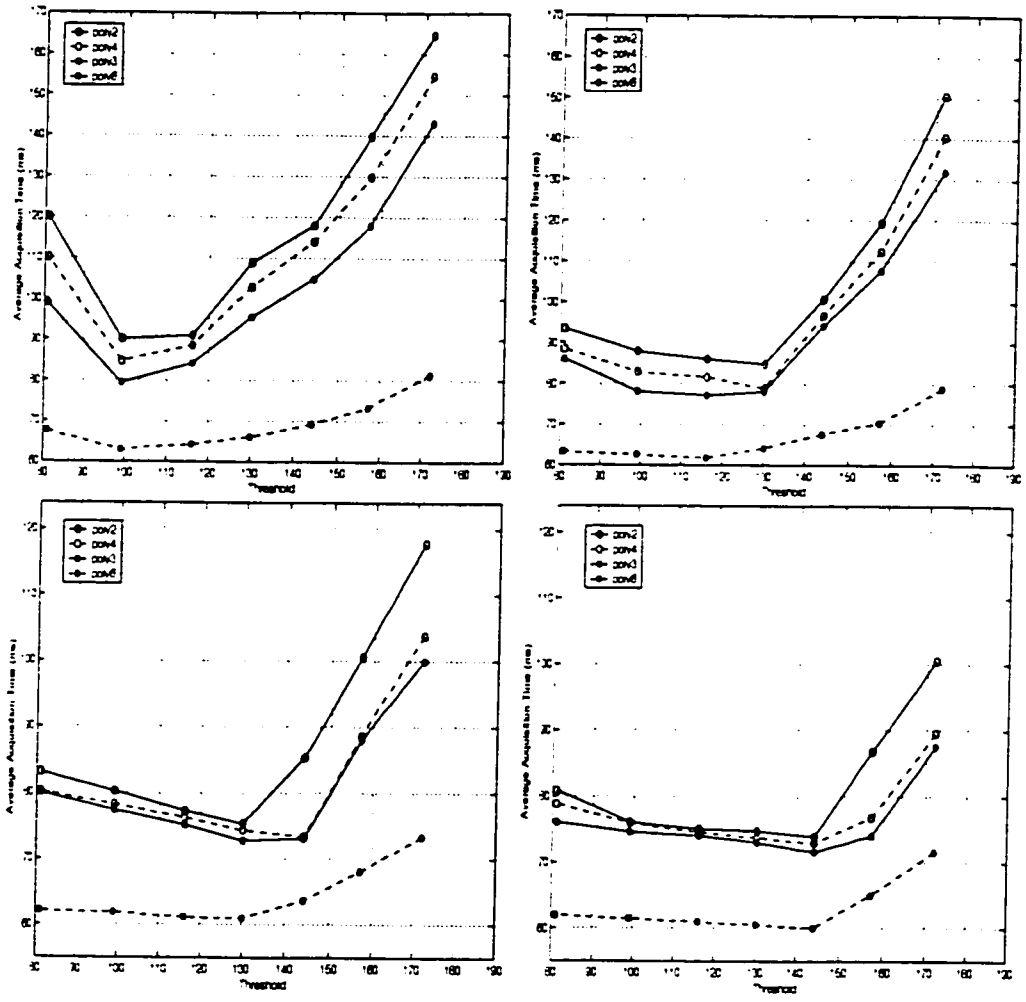

Figure 3.41: Acquisition Time of Different Policies in Flat Fading Channel (8km/h)(SNR=-6,-4,0,2 dB)

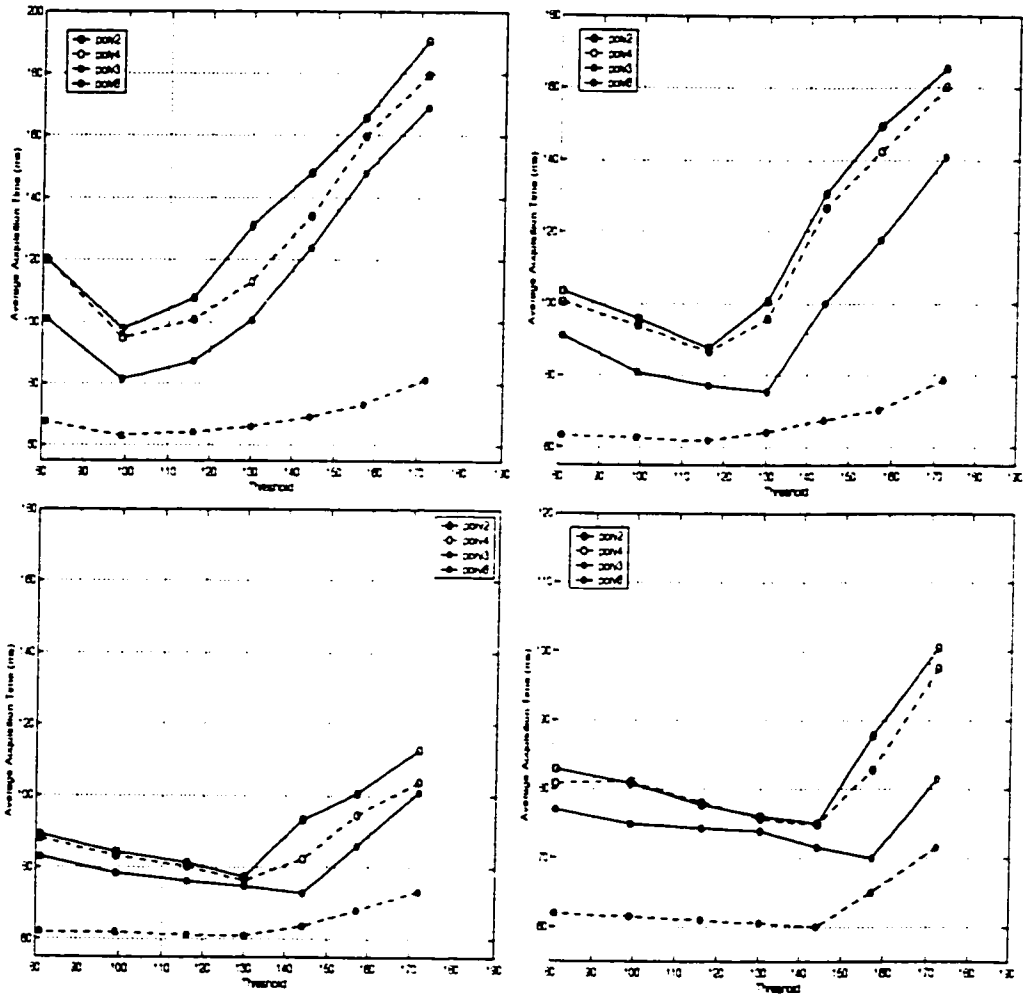

Figure 3.42: Acquisition Time of Different Policies in Flat Fading Channel (80km/h)(SNR=-6,-4,0,2 dB)

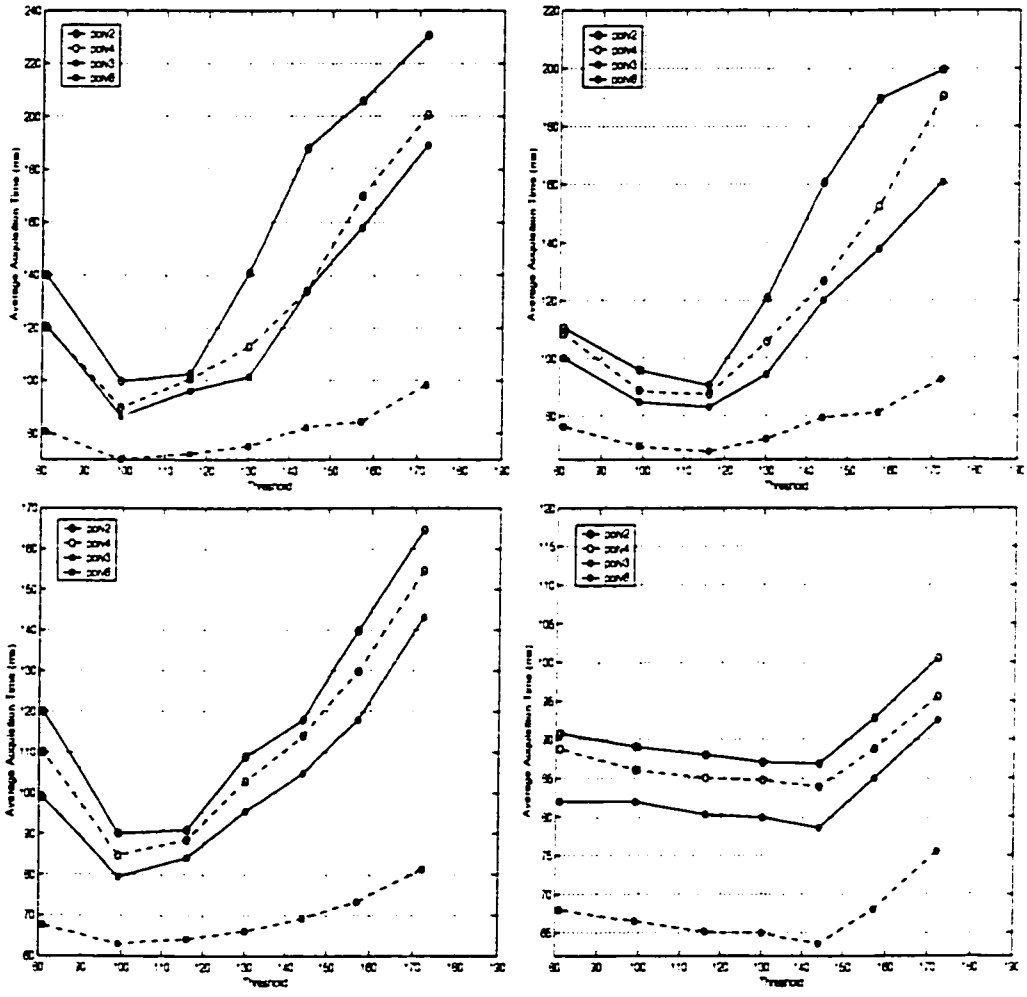

Figure 3.43: Acquisition Time of Different Policies in Frequency-Selective Fading Channel (8km/h)(SNR=-6,-4,0,2 dB)

Chapter 4

Conclusion and Future work

4.1 New algorithms for Code Acquisition In WCDMA

Algorithms for cell search in Wideband CDMA (WCDMA) have been presented. Optimization of key system parameters such as Primary Synchronization (P-SCH) Channel, Second Synchronization Channel (S-SCH), and Common Pilot Channel (CPICH) threshold has been studied. It has been found that the best choice for the CPICH threshold was approximately 99 for the pipelined process considered when G= -6, CPICH threshold is approximately 116 for the pipelined process considered when G= -4, CPICH threshold is approximately 130 for the pipelined process considered when G=0 and CPICH threshold is approximately 144 for the pipelined process considered when G=2. The S-SCH threshold should be in the range (15, 33).

We modified the serial search and obtained Poly1 and Poly2. We also developed the new algorithms: Poly3 and Poly4. As well as the pipelined search Poly5 and Poly6. Poly6 is the new algorithm of cell search. We use the corrector in stage2 based on maximum selection method and the fixed threshold and use the corrector in stage3 based on maximum selection method and the fixed threshold. We change some parameters. At last we get the best performance in our research.The results of

Chapter 3 show that Policy6 yields less average acquisition time than other policies. Policy 4 and Policy3 are better than Policy2 and policy1. Policy3 is an improvement over normal serial search (Policy1.) Policy6 always has the best performance in all four channels. Whatever flat fading channel or frequency-selective channel, Policy6 always has the best performance. Fig 3.36, Fig 3.37, Fig 3.38 and Fig 3.39 show that Policy6 has minimum variance of acquisition time. In this case, the acquisition time of Policy6 changes less than other policies when the SNR changes greatly. Thus Policy6 is the most stable algorithm that was studied.

4.2 Future work

There is much research to continue. First, one can consider the effect of carrier frequency errors. This will have a good effect on code acquisition. Coherent or noncoherent detection could also be compared.

As mentioned in Chapter 3, we could also consider the effects of user load on every channel. One should try to estimate the optimum power on every channel, so as to improve acquisition time.

Bibliography

[1] Malcom W. Oliphant, " The Mobile Phone Meets the Internet," IEEE Spectrum, pp. 20- 28, August 1999.

[2] Tero Ojanpera and Ramjee Prasad, "An Overview of Air Interface Multiple Access for IMT-2000/UMTS," IEEE Communications Magazine, vol. 36, pp. 88-95, September 1998.

[3] Erik Dahlman, Bjorn Gudmundson, Matts Nilsson, and Johan Skold, " UMTS/IMT-2000 Based on Wideband CDMA," IEEE Communications Magazine, vol. 36, pp. 70-80, September 1998.

[4] Erik Dahlman, Per Beming, Jens Knutsson, Fredrik Ovesjo, Magnus Persson, and Christiaan Roobol, " WCDMA- The Radio Interface for Future Mobile Multimedia Communications," IEEE Transactions on Vehicular Technology, vol. 47, No. 4, pp. 1105-1118, November 1998.

[5] Third Generation Partnership Project Technical Specification Group Radio Access Network Working Group 1," Spreading and Modulation," TS 25.213 V2.1.2 (1999-4).

[6] Third Generation Partnership Project Technical Specification Group Radio Access Network Working Group 1, " Physical Channels and Mapping of Transport Channels onto Physical Channels (FDD)," TS 25.211 V2.2.1 (1999-08).

[7] Kevin Laird, Nick Whinnet, and Soodesh Buljore, " A Peak-To-Average Power Reduction Method for Third Generation CDMA Reverse Links," in Proc., IEEE Vehicular Technology Conference, 1999.

[8] Esmael H. Dinan and Bijan Jabbari, "Spreading Codes for Direct Sequence CDMA and Wideband CDMA Cellular Networks," IEEE Communications Magazine, vol. 36, pp. 48- 54, September 1998.

[9] T.S. Rappaport, Wireless Communications: Principles and Practice. Upper Saddle River, NJ: Prentice Hall PTR, 1996.

[10] Third Generation Partnership Project Technical Specification Group Radio Access Network Working Group 1, " Multiplexing and Channel Coding (FDD)," TS 25.212 V2.0.1 (1999-08).

[11] Alpha Concept Group, "Wideband Direct Sequence CDMA (WCDMA) Evaluation Document (3.0)," Tdoc SMG 905/97, December 15-19, 1997, Madrid, Spain.

[12] J. C. Liberti and T.S. Rappaport, Analysis of CDMA Cellular Radio Systems Employing Adaptive Antennas. PhD dissertation, Virginia Tech, Blacksburg, VA, September 1995.

[13] S.M. Alamouti, "A Simple Transmit Diversity Technique for Wireless Communications," IEEE Journal on Selected Areas in Communications, vol. 16, pp. 1451-1458, October 1998.

[14] Texas Instruments, "Space Time Block Coded Transmit Antenna Diversity for WCDMA," ETSI SMG-2 UMTS-L1, TDOC 662/98.

[15] Third Generation Partnership Project Technical Specification Group Radio Access Network Working Group 1, " Physical Layer Procedures (FDD)," TS 25.214 V1.1.2 (1999-08).

[16] Commission of the European Communities, " Digital Land Mobile Radio Communications: COST-207 Final Report," chapter 2, 1988.

[17] W.C. Jakes, Microwave Mobile Communications. John Wiley and Sons, 1974.

[18] R. Price and P.E. Green," A communications technique for multipath channels," Proceedings of the IRE, vol. 2, pp. 555-570, March 1958.

[19] J. G. Proakis, Digital Communications. New York, NY: McGraw-Hill Inc., third ed., 1995.

[20] Roger L. Peterson, Rodger E. Ziemer, and David E. Broth, Introduction to Spread Spectrum Communications. Englewood Cliffs, NJ: Prentice Hall, 1995.

[21] Javier Ramos, Michael D. Zoltowski, and Hui Liu, "A Low-Complexity Space-Time Receiver for DS-CDMA Communications," IEEE Signal Processing Letters, vol. 4, No. 9, pp. 262-265, September 1997.

[22] B. Xu, T.B. Vu, and H. Mehrpour, "A Space-Time Rake Receiver for Asynchronous DS-CDMA System Based on Smart Antenna," in Proc., IEEE Vehicular Technology Conference, 1999.

[23] Babak h. Khalaj, Arogyaswami Paulraj, and Thomas Kailath, "2 D Rake Receivers for CDMA Cellular Systems," in Proc., IEEE Globecom Conference, pp. 400-404, 1994.

[24] T. Ojanperä and R. Prasad, "An overview of air interface multiple access for IMT-2000/UMTS", IEEE Commun. Mag., vol. 36, pp. 8295, Sept.1998.

[25] E. Dahlman, P. Beming, J. Knutsson, F. Ovesjö, M. Persson, and C. Roobol, "WCDMAThe radio interface for future mobile multimedia communications", IEEE Trans. Veh. Technol., vol. 47, pp. 11051118, Nov. 1998.

[26] Yi_pin Eric Wang, Tony Ottosson,"Cell Search in W-CDMA" IEEE Com, pp.1477-1482, August 2000.

[27] 3rd Generation Partnership Project, "Spreading and modulation (FDD)", 3GPP Tech. Spec., TS 25.213, V3.0.0, Oct. 1999.

[28] R. L. Peterson, R. E. Ziemer, and D. E. Borth, "Introduction to Spread Spectrum Communication". Englewood Cliffs, NJ: Prentice-Hall, 1995.

[29] K. Higuchi, M. Sawahashi, and F. Adachi, "Fast cell search algorithm using long code masking in DS-CDMA asynchronous cellular system", AZ, May 1997, pp. 1430-1434.

[30] J. Nyström, K. Jamal, Y.-P. E. Wang, and R. Esmailzadeh, "Comparison of cell search methods for asynchronous wideband CDMA cellular system", in Proc. IEEE 1998 Int. Conf. Universal Personal Commun., Florence, Italy, Oct. 1998.

[31] C. Östberg, Y.-P. E. Wang, and F. Jaenecke, "Performance and com-plexity of techniques for achieving fast sector identification in an asynchronous CDMAsystem", in Proc. 1st Int. Symp. Wireless Personal Multimedia Commun., Japan, Nov. 1998, pp. 8792.

[32] 3rd Generation Partnership Project, "Physical channels and mapping of transport channels onto physical channels (FDD)", 3GPP Tech. Spec., TS 25.211, V3.0.0, Oct. 1999.

[33] Siemens and Texas Instruments, "Generalized hierarchical Golay sequence for PSC with low complexity correlation using pruned efficient Golay correlators", 3GPP Tech. Doc., Tdoc R1-99554, Cheju, Korea, June 1999.

[34] S. Sriram and S. Hosur, "Fast acquisition method for DS-CDMA systems employing asynchronous base stations", in Proc. IEEE Int. Conf. Commun., June 1999.

[35] 3rd Generation Partnership Project, "FDD: Physical layer procedures", 3GPP Tech. Spec., TS 25.214, V3.0.0, Oct. 1999.

[36] 3rd Generation Partnership Project, "UE radio transmission and reception (FDD)", TSG RAN WG4, version 3.0.0, Oct. 1999.

[37] D. C. Rife and R. R. Boorstyn, "Single tone parameter estimation from discrete-time observations", IEEE Trans. Inform. Theory, vol. IT-20, pp. 591-598, Sept. 1964.